

**COMMITTEE CERTIFICATION OF APPROVED VERSION**

The committee for Mimi Leong, MD certifies that this is the approved version of the following thesis:

**EFFECTS OF LIGHT-EMITTING DIODE PHOTOSTIMULATION  
ON BURN WOUND HEALING**

Committee:

---

Lisa J Gould, MD. PhD, Supervisor

---

Linda G. Phillips, MD

---

Hal K. Hawkins, MD, PhD

---

Massoud Motamedi, PhD

---

Gregory K. Asimakis, PhD

---

---

Dean, Graduate School

**EFFECTS OF LIGHT-EMITTING PHOTOSTIMULATION ON  
BURN WOUND HEALING**

by  
Mimi Leong, MD

Thesis  
Presented to the Faculty of The University of Texas Graduate School of  
Biomedical Sciences at Galveston  
in Partial Fulfillment of the Requirements  
for the Degree of

Master of Medical Science

Approved by the Supervisory Committee

Lisa J. Gould, MD, PhD  
Linda G. Phillips, MD  
Hal K. Hawkins, MD, PhD  
Massoud Motamedi, PhD  
Gregory K. Asimakis, PhD

May, 2006  
Galveston, Texas

Key words: angiogenesis, vascular endothelial growth factor, nitric oxide,  
cyclooxygenase-2, wound healing, photostimulation

© 2006, Mimi Leong, MD

To Family, Friends, and Loved Ones

## **ACKNOWLEDGMENTS**

I would like to thank my mentors and all the members of my supervisory committee, but particularly Dr. Lisa Gould and Dr. Linda Phillips for their energy and guidance in affording me the opportunity to contribute to plastic surgical research.

I would like to thank the Division of Plastic Surgery at the University of Texas Medical Branch at Galveston for funding many key aspects of this project. I would also like to thank Fresh Start Surgical Gifts and the Plastic Surgery Educational Foundation for their generous support in the form of the 2002 Research Fellowship and 2002 Research Grant.

Sincere thanks to Dr. Kevin Murphy for his assistance during this project. Thanks to Dr. Ioseb Mushkudiani, Mr. Jiangang Zhao, and Dr. Robert Cox for all their assistance, guidance and help in technical aspects of the project. Finally, a special acknowledgment to Ms. Ann Burke for all her assistance and advice during this project, but who sadly passed away during the writing of this manuscript.

# **EFFECTS OF LIGHT-EMITTING DIODE PHOTOSTIMULATION ON BURN WOUND HEALING**

Publication No. \_\_\_\_\_

Mimi Leong, MMS

The University of Texas Graduate School of Biomedical Sciences at Galveston, 2006

Supervisor: Lisa J. Gould

Annually, more than 1.2 million persons in the United States require medical care for burns. Healing of deep burn wounds requires restored perfusion and neoangiogenesis to reestablish blood flow and limit ischemic damage.

We propose that LED photostimulation, by inducing macrophage proliferation and secretion of pro-angiogenic factors, will restore perfusion by increasing angiogenesis.

An *in vitro* inflammatory model and *in vivo* rodent thermal injury model were treated with LED at 670nm, 730nm, 880nm, or combination-670nm/730nm/880nm. Conditioned media were analyzed for VEGF and NO. Excised burn wounds underwent measurement of surface area, tensile strength, VEGF, nitrites, and immunohistochemical markers (iNOS, VEGF, cyclooxygenase-2, Factor VIII, ED-1) on days 3, 7, and 14.

Both *in vitro* and *in vivo* findings demonstrate that LED therapy has vulnerary effects on angiogenesis, by affecting macrophage production of VEGF and NO. These effects are wavelength and fluence-dependent.

# TABLE OF CONTENTS

	Page
<b>ACKNOWLEDGMENTS .....</b>	<b>IV</b>
<b>LIST OF FIGURES.....</b>	<b>X</b>
<b>LIST OF ILLUSTRATIONS .....</b>	<b>XII</b>
<b>LIST OF ABBREVIATIONS .....</b>	<b>XIII</b>
<b>CHAPTER 1: BURN INJURY AND THE BURN WOUND .....</b>	<b>1</b>
INCIDENCE OF BURN INJURY .....	1
PATHOPHYSIOLOGY OF SEVERE BURN INJURY .....	1
THE BURN WOUND .....	2
<b>CHAPTER 2: PHOTOSTIMULATION .....</b>	<b>4</b>
INTRODUCTION .....	4
MECHANISM OF ACTION .....	4
ADVANTAGES OF LED THERAPY .....	5
EARLY EFFECTS OF LED THERAPY .....	6
<b>CHAPTER 3: WOUND HEALING.....</b>	<b>8</b>
INTRODUCTION .....	8
WOUND HEALING PHASES .....	8
INFLAMMATION.....	8
PROLIFERATION.....	8
MATURATION.....	8

ANGIOGENESIS.....	10
VEGF.....	10
NITRIC OXIDE.....	10
NO AND VEGF INTERACTIONS.....	13
MACROPHAGES IN WOUND HEALING.....	14
CYCLOOXYGENASE -2 (COX-2).....	16
NO AND COX-2 INTERACTIONS.....	17
NO, VEGF, AND COX-2 INTERACTIONS.....	17
<b>CHAPTER 4: AIMS AND HYPOTHESES.....</b>	<b>19</b>
CENTRAL HYPOTHESES.....	19
SPECIFIC AIMS.....	19
<b>CHAPTER 5: MATERIALS AND METHODS.....</b>	<b>21</b>
STUDY TYPE AND DESIGN.....	21
IN VITRO MODEL.....	21
ANIMAL MODEL.....	21
CELL CULTURE.....	21
RATIONALE.....	21
CELL TREATMENT.....	21
BURN WOUND ANIMAL MODEL.....	22
ANIMALS AND ENVIRONMENT.....	23
ANESTHESIA AND ANALGESIA.....	23
BURN PROCEDURE (CONTACT BURN MODEL).....	24

EUTHANASIA.....	24
LED TREATMENT.....	24
LIGHT SOURCES .....	24
SACRIFICE.....	25
PLANIMETRY .....	25
BURN WOUND ZONE ENRICHMENT .....	25
TENSIOMETRY .....	25
TISSUE HOMOGENIZATION.....	25
VEGF ANALYSIS .....	28
NITRITE ANALYSIS (GREISS REACTION .....	28
MACROPHAGE PROLIFERATION .....	29
LIGHT MICROSCOPY .....	29
IMMUNOHISTOCHEMISTRY .....	30
<b>CHAPTER 6: RESULTS .....</b>	<b>32</b>
PLANIMETRY .....	32
TENSIOMETRY .....	33
VEGF LEVELS.....	34
NITRITE LEVELS.....	35
LIGHT MICROSCOPY .....	36
IMMUNOHISTOCHEMISTRY .....	37
<b>CHAPTER 7: DISCUSSION .....</b>	<b>59</b>
EFFECTS OF LED ON BURN WOUND – PREVIOUS STUDIES.....	59

TEMPERATURE – INDUCED EFFECTS ON LED STUDIES .....	59
EFFECT OF WAVELENGTH ON WHOLE BURN WOUNDS .....	60
EFFECT OF WAVELENGTH ON BURN WOUND ZONES .....	62
EFFECT OF WAVELENGTH ON MACROPHAGE PRODUCTION OF VEGF AND NO IN VITRO.....	64
<b>CHAPTER 8: CONCLUSIONS.....</b>	<b>69</b>
<b>CHAPTER 9: BIBLIOGRAPHY.....</b>	<b>70</b>

## LIST OF FIGURES

FIGURE 1: LED Light sources – A) example of 670nm and 880nm wavelength LED light sources, B) Spectral outputs for 670nm, 730nm, and 880nm wavelength LEDs

FIGURE 2: Wound surface area on postburn day 14. Combination (combo) LED-treated wounds were approximately 1 cm<sup>2</sup> smaller than wounds of other groups. N=3 per treatment group.

FIGURE 3: Tensiometry at postburn day 3, 7, and 14. N=3 per treatment group.

FIGURE 4: VEGF levels at postburn days 3, 7, and 14 in whole wound homogenates compared to control (no LED) rats. N=3 per treatment group.

FIGURE 5: Nitrite levels at postburn days 3, 7, and 14 in whole wound homogenates compared to control (no LED) rats. N=3 per treatment group.

FIGURE 6: iNOS immunohistochemistry. A) iNOS antibody localized to the inflammatory cell layer in the burn wound. B) iNOS positive area in postburn day 7 burn wounds. N=9 per treatment group.

FIGURE 7: VEGF immunohistochemistry. A) VEGF antibody localized to macrophage-like cells in the burn wound. B) VEGF positive area in postburn day 7 burn wounds. N=6 per treatment group.

FIGURE 8: Factor VIII immunohistochemistry. A) Factor VIII antibody localized to luminal structures containing red blood cells. B) Factor VIII positive blood vessels in postburn day 7 burn wounds. N=9 per treatment group.\* p < 0.05 combination treatment compared to control (no LED).

FIGURE 9: COX-2 immunohistochemistry in LED-treated groups. COX-2 expression in postburn day 14 burn wounds. N=3 per treatment group; \*p<0.01 670 nm vs. control (no LED).

FIGURE 10: A) ED-1 (top left) and iNOS (bottom left) immunohistochemistry (40x magnification). iNOS and ED-1 antibodies localized to macrophages in the burn wound. B) ED-1 (top center) and VEGF (bottom center) immunohistochemistry (40x magnification). VEGF and ED-1 antibodies localized to macrophages in the burn wound. C) ED-1 (top right) and COX-2 (bottom right) immunohistochemistry (40x magnification). COX-2 and ED-1 antibodies localized to macrophages in the burn wound.

FIGURE 11: Pro-angiogenic factors in the different burn wound zones at postburn day 7.

A) VEGF levels B) Nitrite levels.

FIGURE 12: Immunohistochemistry summary – rat skin (1x magnification).

FIGURE 13: Effect of LED treatment on VEGF levels in LPS/IFN stimulated and non-stimulated macrophages. The nonLPS/IFN stimulated (serum-starved) cells are on the left side of the graph and the LPS/IFN stimulated cells on the right side of the graph. (\* $p < 0.05$ , combination versus control in nonLPS/IFN stimulated)  $N=3/\text{treatment}$ . VEGF levels are expressed as mean pg/ml  $\pm$  SEM.

FIGURE 14: Effect of LED treatment on nitrite levels in LPS/IFN stimulated and non-stimulated macrophages. The nonLPS/IFN stimulated (serum-starved) cells are the left side of the graph and the LPS/IFN stimulated cells on the right side of the graph. (\* $p < 0.05$ , 730 nm versus others in LPS/IFN stimulated)  $N=3/\text{treatment}$ . Nitrite levels are expressed as mean  $\mu\text{M} \pm$  SEM.

FIGURE 15: Effect of LED treatment on nitrite levels in nonLPS/IFN stimulated macrophages. (\* $p < 0.05$ , 880 nm and combination versus 730 nm)  $N=3/\text{treatment}$ . Nitrite levels are expressed as mean  $\mu\text{M} \pm$  SEM.

FIGURE 16: Correlation of nitrite levels to VEGF in nonLPS/IFN stimulated and LPS/IFN stimulated macrophages. The left hand set of points represents the nonstimulated cells and the right hand set represents the LPS/IFN stimulated cells. There is a direct positive correlation between nitrites (an indirect measure of NO) and VEGF. The slope of the line for the nonLPS/IFN stimulated cells is four-fold greater than that of the LPS/IFN stimulated cells.

FIGURE 17: Effect of LED treatment on macrophage proliferation in nonLPS/IFN stimulated and LPS/IFN stimulated cells. LPS/IFN stimulation resulted in 25% decrease in macrophage proliferation in all LED-treated groups compared to control (\* $p < 0.05$ , all LED-treatment groups versus control in LPS/IFN stimulated cells)  $N=3/\text{treatment group}$ . Proliferation expressed as mean OD  $\pm$  SEM.

## **LIST OF ILLUSTRATIONS**

ILLUSTRATION 1: Burn wound zones – zone of coagulation, zone of stasis, zone of hyperemia

ILLUSTRATION 2: Phases of wound healing – inflammation (a), proliferation (b). Maturation phase not shown. (From Leong M, Phillips LG. Wound Healing. In: Townsend, Beauchamp, Evers, & Mattox eds: Sabiston Textbook of Surgery: The Biological Basis of Modern Surgical Practice. 17th edition, Philadelphia, Saunders (Elsevier Science), 2004: 183-207.)

ILLUSTRATION 3: Nitric Oxide Synthesis

ILLUSTRATION 4: Central role of the macrophage in wound healing. (From Leong M, Phillips LG. Wound Healing. In: Townsend, Beauchamp, Evers, & Mattox eds: Sabiston Textbook of Surgery: The Biological Basis of Modern Surgical Practice. 17th edition, Philadelphia, Saunders (Elsevier Science), 2004: 183-207.)

ILLUSTRATION 5: Interactions of NO, VEGF, and COX-2

ILLUSTRATION 6: Schemata of rat burn model

## LIST OF ABBREVIATIONS

LELL	Low Energy Laser Light
LED	Light-Emitting Diode
VEGF	Vascular Endothelial Growth Factor
NO	Nitric Oxide
COX-2	Cyclooxygenase-2
TNF- $\alpha$	Tumor Necrosis Factor – alpha
IFN- $\gamma$	Interferon – gamma
LPS	Lipopolysaccharide
DNA	Deoxyriboneuclide
iNOS	inducible nitric oxide synthase
VEGFR-1	VEGF receptor 1 also Flt-1
VEGFR-2	VEGF receptor 2 also KDR
TBSA	total body surface area
IL-1	Interleukin-1
Cu	Copper
PMN	Polymorphonuclear neutrophil
NOS	Nitric oxide synthase
UV	Ultraviolet
cGMP	cyclic Guanosine monophosphate
cAMP	cyclic Adenosine monophosphate
PGE <sub>2</sub>	Prostaglandin E <sub>2</sub>

LPS	Lipopolysaccharide
DMEM	Dulbecco's Modified Eagle's Medium
CO <sub>2</sub>	Carbon dioxide
ELISA	Enzyme-linked immunosorbent assay
NO <sub>2</sub>	nitrite
NO <sub>3</sub>	nitrate
NADH	Nicotinamide adenine dinucleotide (reduced form)
H <sub>2</sub> O <sub>2</sub>	hydrogen peroxide
DAB	3,3'-Diaminobenzidine
ED1	monoclonal specific rat macrophage marker
HPF	high-power field
Factor VIII	Factor Eight
PBD	Post Burn Day
PGI <sub>2</sub>	Prostacyclin
L-NIL	L-N6- (1-iminoethyl) lysine
J/cm <sup>2</sup>	Joules per square centimeter
nm	nanometer
mm	millimeter
cm	centimeter
HUVEC	human umbilical vein endothelial cells
N	Newton

ONOO<sup>-</sup>

Peroxynitrite

SOD

superoxide dismutase

# **CHAPTER 1: BURN INJURY AND THE BURN WOUND**

## **INCIDENCE OF BURN INJURY**

Annually, more than 1.2 million persons in the United States require medical care for burns, with 3,900 people dying of burn-related complications (Brigham, 1996). Recently, because of advances in burn care, patients with large body surface area burns are surviving (Herndon, 2001). The improved survival rates and decreased wound infection rates have resulted in a 50% decline in burn related deaths and hospital admissions in the United States (Brigham, 1996). Massive burn injury, however, still results in extensive wounds with limited options for coverage and poor functional outcomes secondary to scarring and delayed wound healing. Improved outcomes in terms of reduced burn scar contracture, reduced hypertrophic scarring and elimination of chronic wounds requires rapid healing of donor sites, grafted areas and the burn wound itself.

## **PATHOPHYSIOLOGY OF SEVERE BURN INJURY AND THE INFLAMMATORY RESPONSE**

Severe thermal injury releases multiple inflammatory mediators that induce numerous physiologic and immunologic alterations. Elevated levels of mediators, such as IL-1, and TNF- $\alpha$  have been demonstrated in the plasma of burned patients (Barbul, 1992, Shakespeare, 2001, Yamada, 1996, Vindenes, 1998, Andrzejewska, 2000, Zhang, 1998). More pronounced elevations of these proinflammatory mediators have also been demonstrated following invasive infection of the burn wound (Chai, 2000, Klein, 2000). These cytokines play an important role in the pathogenesis of burn sepsis; surgical debridement of the infected burn wound has been shown to decrease plasma levels of these cytokines and improve the patient's condition (Chai, 2000). Subsequently, early excision and grafting has been advocated as an important component in the care of the burn-injured patient.

## **THE BURN WOUND**

Classically, the burn wound is composed of three zones of injury: coagulation, stasis and hyperemia (Boykin, 1992, Shakespeare, 2001, Zawacki, 1974). Coagulation of skin blood vessels causes irreversible skin death. Surrounding this zone is an area in which blood flow may be limited to the point of stasis. At the edge of the injured area, the interface between burned and unburned skin, is an area in which there is hyperemia (Shakespeare 2001) (Illustration 1). Each zone reflects varying levels of ischemia that responds to treatment differently. Little can be done for the zone of coagulation because it is already necrotic and little needs to be done for the zone of hyperemia because it will heal on its own. The zone of stasis, however, has the potential to either heal or become necrotic. Thus, the final size of the burn wound depends upon the fate of the zone of stasis, which is an area of marginal perfusion.

Both systemic and local factors can affect the zone of stasis. Studies in burn wound models have shown that both systemic and local factors alter perfusion of burned tissues (Boykin, 1980, Robson, 1979). deCamara et al demonstrated in guinea pigs with partial thickness scald burns that there was a definite progression of thermal injury, with maximal tissue destruction occurring eight hours after the burn (deCamara, 1982). This progressive dermal ischemia could be decreased by treatment with anti-inflammatories, such as the thromboxane (TxA<sub>2</sub>) inhibitors, imidazole, methimazole, and dipyridamole (Robson 1980). Interestingly, levels of PGE<sub>2</sub> and PGI<sub>2</sub> in treated animals were the same as in untreated controls, but the anti-thromboxane treated animals had increased dermal perfusion to their burn wounds, as demonstrated by Xenon133 washout studies (Robson 1980).

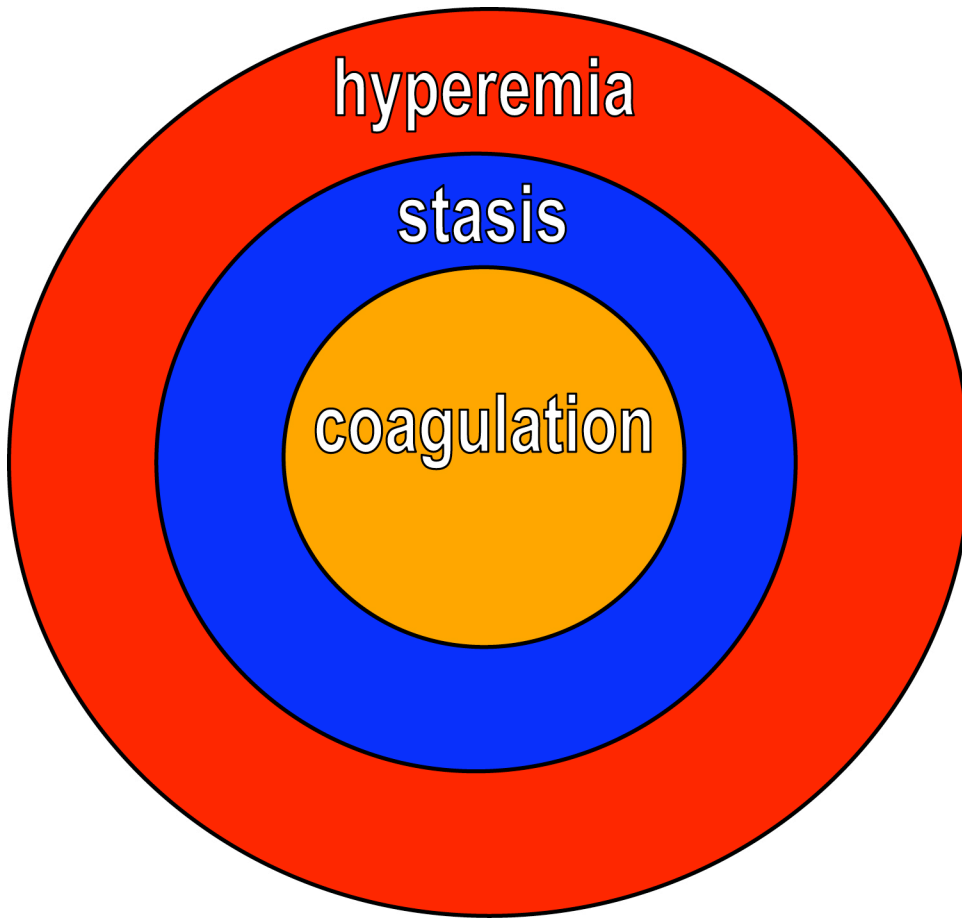


ILLUSTRATION 1: Burn wound zones – zone of coagulation, zone of stasis, zone of hyperemia

## **CHAPTER 2: PHOTOSTIMULATION**

### **INTRODUCTION**

Photostimulation is the use of light to artificially activate biological compounds, cells, or even whole organisms (Karu 1989). Photostimulation, using low energy laser light (LELL) and more recently, light-emitting diodes (LEDs) (Figure 1), has been utilized to modulate wound healing. Studies have associated improvements in wound healing with wavelengths in the red and infrared range (Karu, 1989, Mester, 1971, Conlan, 1996), in the range of 450 nm - 750 nm. At these wavelengths, photostimulation has been demonstrated to increase fibroblast proliferation, growth factor production, collagen and other matrix protein synthesis and stimulate macrophage function (Conlan, 1996, Karu, 1989).

### **MECHANISM OF ACTION**

The mechanisms by which LELL and LEDs mediate their effects are poorly understood. It has been postulated that laser biostimulation occurs at the mitochondrial level, causing redox regulation of cellular metabolism at low doses and specific wavelengths. However, the photoacceptors that respond to light stimulation have not been determined. Current evidence suggests that molecules in the mitochondrial electron transport chain, particularly cytochrome c oxidase, are affected by photostimulation (Wong-Riley, 2005, Eells JT 2004).

Cytochrome c oxidase is the terminal enzyme of the electron transport chain of all eukaryotes, oxidizing its substrate cytochrome c and reducing molecular oxygen to water. It is an important energy-generating enzyme critical for proper functioning of almost all cells. Fifty percent of near-infrared light is absorbed by mitochondrial chromophores such as cytochrome c oxidase (Wong-Riley, 2001). Cytochrome oxidase is an integral membrane protein and contains four redox active metal centers: the dinuclear  $\text{Cu}_A$ ,  $\text{Cu}_B$ , heme a and heme  $a_3$ , all of which have absorbance in the red to near-infrared range detectable in vivo by near-infrared spectroscopy

(Wong-Riley, 2001). In the process of taking four reducing equivalents from cytochrome c and converting molecular oxygen to water, cytochrome c oxidase translocates protons, helping to establish a chemiosmotic potential that the ATP synthase then uses to synthesize ATP.

Cytochrome c is a small heme protein that is highly conserved across species and found in plants, animals, and many unicellular organisms. Cytochrome c is found loosely associated with the inner membrane of the mitochondrion and is an essential component of the electron transfer chain. Cytochrome c is capable of undergoing oxidation and reduction, but does not bind oxygen. It transfers electrons between Complexes III and IV of the electron transport chain. Interestingly, cytochrome c is also an intermediate in apoptosis, which is a controlled form of cell death used to kill cells in the process of development or in response to infection or DNA damage.

It is thought that LELL and LED therapy increase activity of cytochrome c, thereby increasing metabolic activity and freeing up more energy for the cells to repair the tissue. The mechanism of this increased activity is not well understood, but the absorption of light by cytochrome c oxidase may induce signaling events related to increased oxidative metabolism and increased generation of reactive oxygen species (Eels, 2004).

### **ADVANTAGES OF LED THERAPY**

Compared to LELL, LED technology provides a more efficient, less expensive, non-thermal optical source of low energy photons in a wider variety of wavelengths. LEDs have also been deemed a nonsignificant risk by the FDA, and the FDA has approved the use of LEDs in human for light therapy. Because LED therapy is non-contact and atraumatic, it could be a beneficial therapeutic modality for patients with massive burn injury who have extensive

wounds, potentially sparing them from repeated trips to the operating room and the pain and systemic alterations associated with surgical interventions.

### **EARLY EFFECTS OF LED THERAPY**

Near infrared photostimulation, using LEDs at 680 nm, 730 nm, and 880 nm resulted in enhanced DNA synthesis in cultured fibroblasts and muscle cells, as well as improved healing of wounds in diabetic mice (Whelan, 2001). Effects of LED appear to be specific to cell growth phase, with beneficial effects occurring within twenty-four hours after LED photostimulation (Reddy, 2001).

Although these studies have shown stimulatory effects on cells and growth factor production in the proliferative phase of wound healing, the effect of LED photostimulation on other components of the proliferative phase, such as angiogenesis has not been clearly elucidated. Angiogenesis, the process of new blood vessel formation, is an essential component of the proliferative phase of wound healing. Increased angiogenesis should result in accelerated wound healing, particularly in wounds, such as burns, where tissue ischemia is an important component.

**A**



**B**

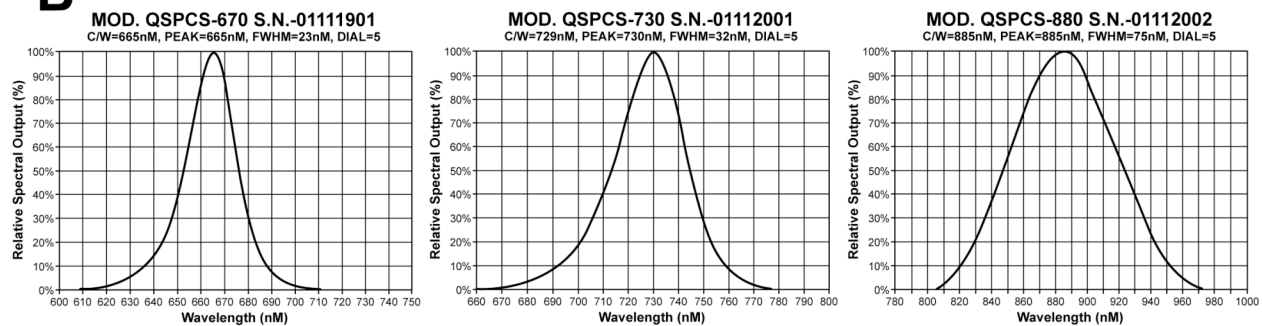


FIGURE 1: LED Light sources – A) example of 670nm and 880nm wavelength LED light sources, B) Spectral outputs for 670nm, 730nm, and 880nm wavelength LEDs

## CHAPTER 3: WOUND HEALING

### INTRODUCTION

Wound healing involves a complex process of cellular interactions coordinated by cytokines and growth factors leading to restoration of tissue integrity. Normal wound healing is characterized by three phases: inflammation, proliferation, and maturation (remodeling) (reviewed in Leong, 2005) (Illustration 2).

### WOUND HEALING PHASES

#### Inflammation

In the *inflammatory* phase, the body responds to injury, such as a burn, by immediately limiting the amount of damage and preventing further injury. The inflammatory phase is characterized by hemostasis and vasoconstriction followed by vasodilation and increased vascular permeability as host defense cells, such as polymorphonuclear cells (PMNs) and macrophages rapidly move into the wounded area. These cells quickly clear bacteria and debris and secrete cytokines and growth factors to prepare for the second phase of wound healing. As the acute responses of hemostasis and inflammation begin to resolve, the scaffolding is laid for repair of the wound with angiogenesis, fibroplasia, and epithelialization.

#### Proliferation

The *proliferative* phase is characterized by reepithelialization, matrix synthesis, and angiogenesis (or neovascularization) to relieve the ischemia of the trauma itself. In this stage, granulation tissue formation occurs. Granulation tissue consists of a capillary bed, fibroblasts, macrophages, and a loose scaffold of collagen, fibronectin, and hyaluronic acid.

#### Maturation

The final *maturational* (or remodeling) phase is the period of scar contraction with collagen cross-linking, shrinking, and a loss of edema. In a large wound such as a burn wound,

the eschar or fibrinous exudate represents the inflammatory phase; the granulation tissue is part of the proliferative phase; the contracting or advancing edge is part of the maturational phase. All three phases may occur simultaneously, and the phases with their individual processes may overlap.

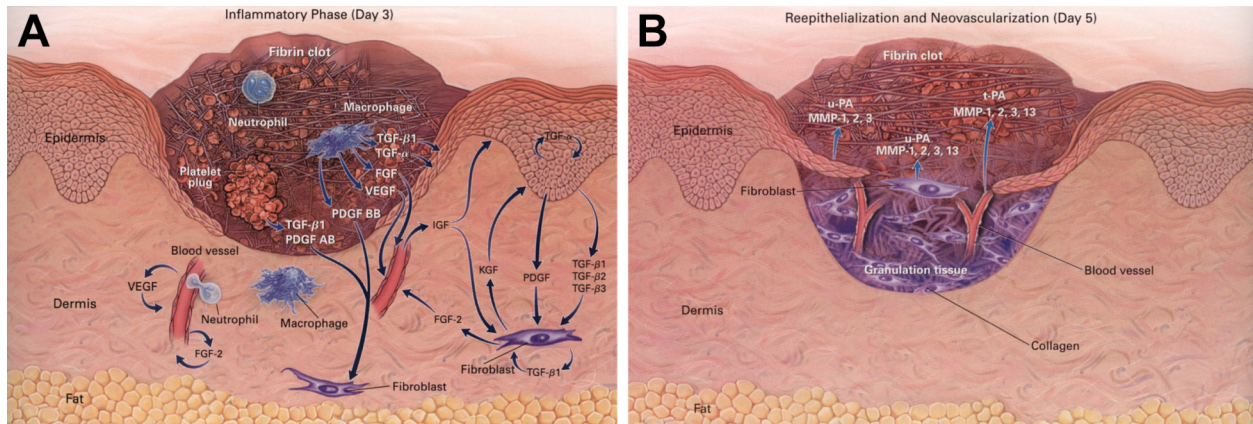


ILLUSTRATION 2: Phases of wound healing – inflammation (a), proliferation (b). Maturation phase not shown. (From Leong M, Phillips LG. Wound Healing. In: Townsend, Beauchamp, Evers, & Mattox eds: Sabiston Textbook of Surgery: The Biological Basis of Modern Surgical Practice. 17th edition, Philadelphia, Saunders (Elsevier Science), 2004: 183-207.)

## **ANGIOGENESIS**

Angiogenesis, as an important component of the proliferative phase, has the potential to change the fate of the zone of stasis. The process of capillary tube formation is complex and requires both endothelial and macrophage interactions and is dependent upon the surrounding matrix. This process is stimulated and manipulated by macrophage and platelet derived cytokines. Although numerous factors have been demonstrated to be involved in angiogenesis, vascular endothelial growth factor (VEGF), nitric oxide (NO), and cyclooxygenase-2 (COX-2) have also been implicated in wound healing (Dulak, 2000, Futagami, 2002, Jones, 1999, Papapetropoulos, 1997, Whelan, 2000) and appear to be interrelated (Dulak, 2000, Papapetropoulos, 1997, Frank, 1999).

### **VEGF**

VEGF's role in angiogenesis has been well documented. It is a potent growth factor that acts on endothelial cells to promote proliferation and differentiation. Cell disruption and hypoxia, which occur following tissue injury, serve as strong initial inducers of VEGF (Detmar, 1997). VEGF is produced in large amounts by several cell types including macrophages, and serves to propagate the angiogenic response (Nwometh, 1997, Witte, 1997).

### **Nitric Oxide (NO)**

Nitric oxide's role as a gaseous free radical responsible for bactericidal cell killing and its relaxant effect on vascular smooth muscle have long been recognized. Nitric oxide is produced by many cell types in the skin, and is formed by the conversion of the amino acid, L-arginine to L-citrulline and nitric oxide, mediated by the enzymatic action of nitric oxide synthase (NOS) (Levy 2005) (Illustration 3). NOS exists as three forms, but the "inducible" form is produced in large amounts by neutrophils and macrophages upon stimulation (Witte, 1997). iNOS is not

expressed under basal conditions, except in intestinal, bronchial, and renal tubular epithelium. Rather, iNOS expression occurs in the face of cellular distress and inflammation caused by a variety of factors, including circulating proinflammatory cytokines, microbial components (endotoxin), mechanical shear stress, hypoxia, and oxidative stress, as occurs in sepsis or shock (Levy, 2005). The regulation of iNOS expression is thought to occur primarily at the level of gene expression. iNOS expression results in sustained production of large quantities of NO for extended periods of time. Thus, iNOS generated NO can lead to sustained vasodilatation or cell toxicity and subsequently can contribute to the pathophysiology of inflammation, sepsis, and shock.

Nitric oxide has emerged as a ubiquitous signaling molecule with prominent roles in maintaining homeostasis and contributing to the pathogenesis of acute and chronic illness. The diversity of biological functions attributed to this simple molecule include roles as signaling messenger, cytotoxin, antiapoptotic agent, antioxidant, and regulator of microcirculation. More recently, NO's multiple roles in angiogenesis and in dermal wound healing have become increasingly apparent (Papapetropoulos 1997, Dulak, 2000).

# Nitric Oxide Synthesis

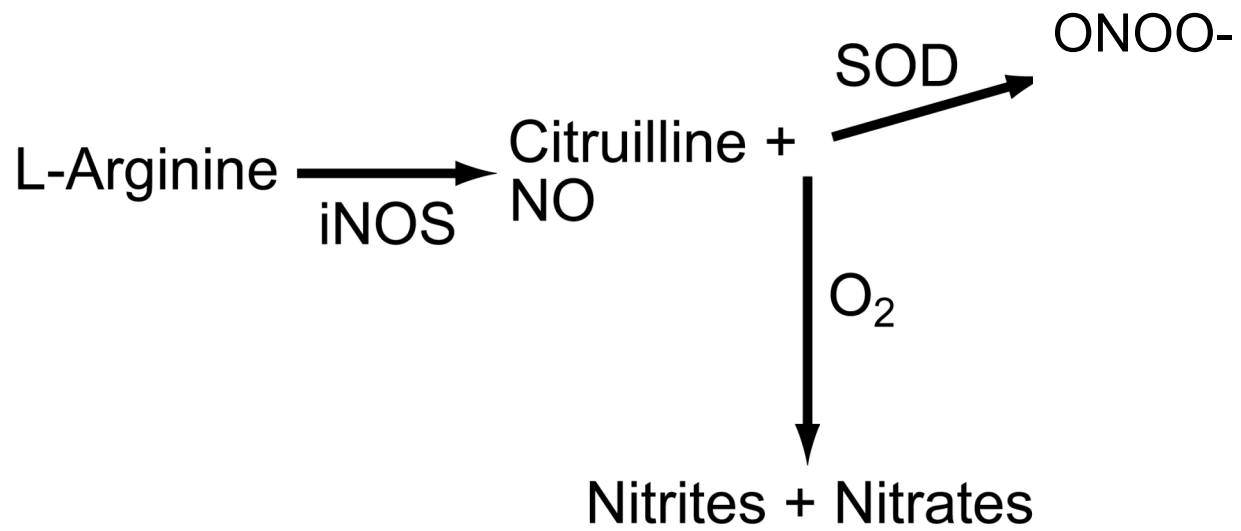


ILLUSTRATION 3: Nitric oxide synthesis

### ***NO and VEGF interactions***

Wound healing studies have demonstrated an interaction between NO and VEGF. Nitric oxide may be required to mediate production of VEGF. Studies with iNOS knockout mice have demonstrated that decreased iNOS expression resulted in decreased VEGF. This resulted in decreased proliferative changes which adversely affected wound healing (Most, 2001). Most et al. (Most, 2001) demonstrated lower levels of VEGF expression in iNOS knockout mice compared to wild type mice in a model of skin graft healing; these animals had elevated levels of the proinflammatory cytokine tumor necrosis factor- $\alpha$  (TNF- $\alpha$ ) which may be in response to a lack of functional iNOS enzyme. As a result, skin grafts of iNOS knockout mice had greater inflammatory changes than their wild-type counterparts (Most, 2001). The authors concluded that these changes were consistent with persistence of the inflammatory phase of wound healing and were due to impaired nitric oxide production, suggesting a role for NO in angiogenesis and progression to normal wound healing.

VEGF has also been shown to upregulate NO synthesis, which may be required to assist with the intracellular VEGF signal transduction necessary for proliferating endothelial cells. NO has been shown to be a negative regulator of vascular endothelial growth factor receptor-2 (VEGFR-2) or (KDR)-mediated proliferation and to promote endothelial cell differentiation (Bussolati 2001). Akcay et al. (Akcay, 2000) demonstrated that inhibition of NO reduced epithelial proliferation, collagen formation, and granulation tissue in mouse burn wounds. This confirmed the necessity of the presence of sufficient NO in order for normal wound healing to proceed (Akcay, 2000). The results of these studies suggest that the regulation of NO and VEGF are interdependent.

## **MACROPHAGES IN WOUND HEALING**

Although there have been numerous studies investigating the role of NO in inducing VEGF, the data on NO-mediated regulation of VEGF in macrophages is limited. Macrophages play a central role in wound healing, participating in debridement of the wound during the inflammatory phase as well as secretion of multiple cytokines necessary to move into the proliferative phase and angiogenesis (Illustration 4). Macrophages are important sources of VEGF and NO in healing wounds (Crowther, 2001) and likely play a key role in the angiogenic response.

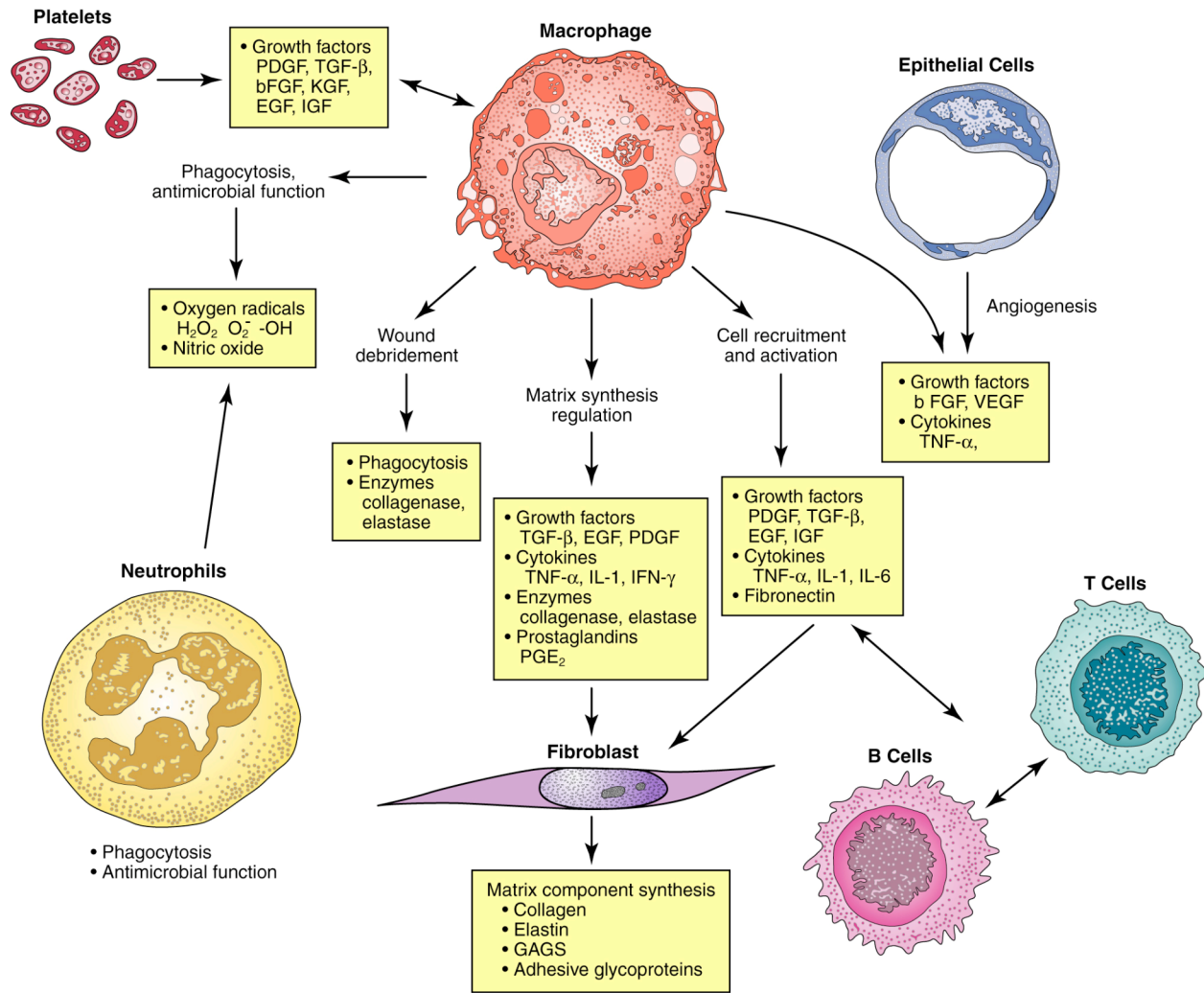


ILLUSTRATION 4: Central role of the macrophage in wound healing. (From Leong M, Phillips LG. Wound Healing. In: Townsend, Beauchamp, Evers, & Mattox eds: Sabiston Textbook of Surgery: The Biological Basis of Modern Surgical Practice. 17th edition, Philadelphia, Saunders (Elsevier Science), 2004: 183-207.)

## **Cyclooxygenase-2 (COX-2)**

Recently, cyclooxygenase-2 (COX-2) has also been implicated in angiogenesis (Jones, 1999). Prostaglandins and other eicosanoids are produced during inflammation, mediated by COX-2, which has been localized to macrophages (Kampfer, 2003). COX-2 is highly expressed in tumors, such as human colon carcinoma, squamous cell carcinoma of the esophagus, and skin cancer (Fosslien, 2000) and is believed to contribute to angiogenesis and subsequent metastatic potential of these tumors. In a breast cancer progression study, treatment with the COX-2 inhibitor, indomethacin, resulted in decreased microvessel density (Raspollini, 2004).

Other studies have also demonstrated the importance of COX-2 in wound healing (Futagami 2002). COX-2 protein and mRNA were expressed mainly within the basal layer of the epidermis, peripheral cells in the outer root sheath of hair follicles, and fibroblast-like cells and capillaries near epidermal wound edges, and administration of a COX-2 inhibitor delayed reepithelialization in early wound healing and impaired angiogenesis (Futagami 2002). Since the epidermis serves as a physical barrier to prevent fluid loss and bacterial invasion, expedient reepithelialization of the skin after wounding is an important step to maintain the body's defenses.

However, the effect of COX-2 on the epithelium is not clear. Epithelialization involves a sequence of changes in wound keratinocytes: detachment, migration, proliferation, differentiation, and stratification. One study showed that COX-2 inhibition delayed reepithelialization in the early phase of wound healing and also inhibited angiogenesis (Futagami, 1992). Another study showed that neither selective COX-2, nor nonselective COX inhibition altered keratinocyte proliferation and differentiation, dermal angiogenesis, or the recovery of wound tensile strength (Blomme, 2003).

Despite these conflicting studies, there is evidence to suggest that COX-2 expression can

be induced in the basal keratinocyte layer. One such stimulus is photostimulation in the form of acute ultraviolet (UV) exposure. Following acute UV exposure, COX-2 expression was predominantly induced in the basal keratinocyte layer. This induction was coincident with an increase in keratinocyte proliferation and apoptosis. Further investigation using the selective COX-2 inhibitor, SC-791 and the traditional nonsteroidal COX inhibitor, indomethacin resulted in decreased UVA and UVB-induced epidermal keratinocyte proliferation. Interestingly, keratinocyte apoptosis was increased with COX-2 inhibition of these UVA- and UVB-damaged basal keratinocytes. These results suggested to the authors that COX-2 expression was necessary for keratinocyte survival and proliferation after acute UV irradiation and that selective COX-2 inhibition would lead to enhanced removal of UV-damaged keratinocytes, decreasing malignant transformation in the epidermis (Tripp, 2003).

#### ***NO and COX-2 interactions***

Recent evidence suggests that an interrelationship between COX-2 and iNOS exists. NO donors enhance COX-2 expression (Salvemini, 1996), which in turn, upregulate VEGF production, leading to increased angiogenesis (Miura, 2004). Conversely, inhibition of COX-2 results in decreased angiogenesis (Fife, 2004). Interestingly, the effect of NO on COX-2 activity is cGMP-mediated (Tetsuka 1996), whereas PGE<sub>2</sub> enhances iNOS activity via generation of cAMP. NOS inhibitors block LPS stimulated PGE<sub>2</sub> production (Salvemini, 1995) while NO donors potentiate arachidonic acid-induced inflammation (Sautebin 1995). PGE<sub>2</sub> increase macrophage iNOS activity in response to IFN- $\gamma$  (Mullet 1997) or TNF- $\alpha$  and IFN- $\gamma$  (Mauel 1995).

#### ***NO, VEGF, and COX-2 Interactions***

In summary, evidence exists that NO, VEGF, and COX-2 are interdependent. NO induces both VEGF and COX-2 production, which, in turn, results in increased angiogenesis. The

various interrelationships between these macrophage-derived growth factors and mediators underscore the delicate balance that must be maintained both in angiogenesis and wound healing (Illustration 5).

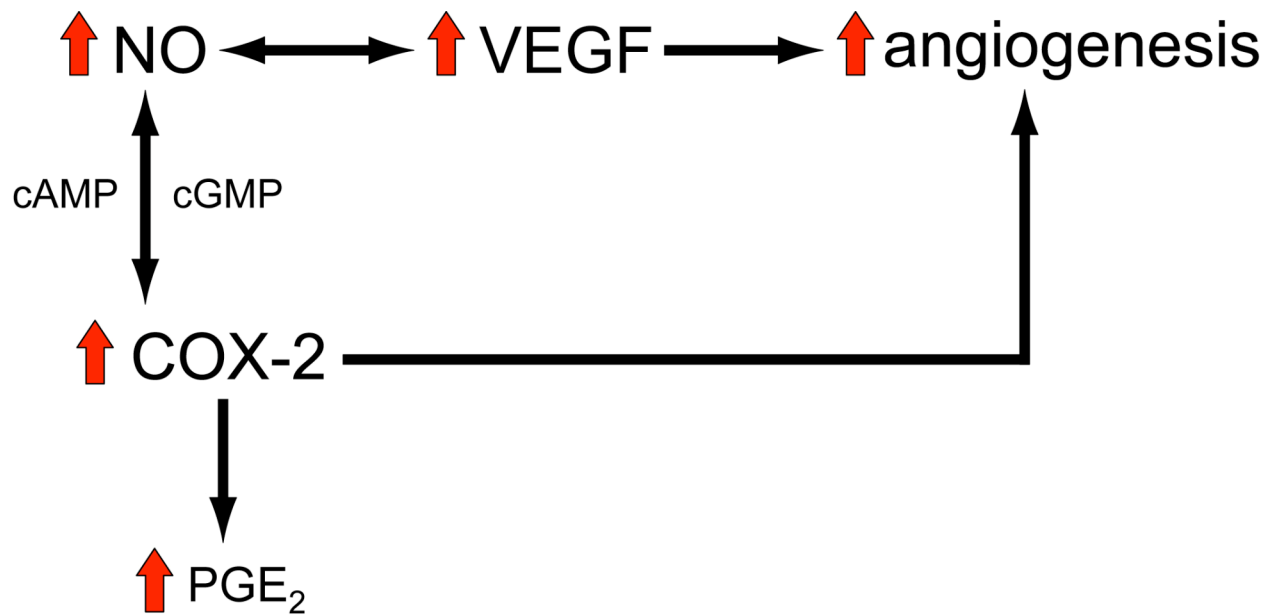


ILLUSTRATION 5: Interactions of NO, VEGF, and COX-2

## **CHAPTER 4: AIMS AND HYPOTHESES**

Burn wounds are associated with varying degrees of tissue ischemia with potential progression of the zone of stasis to necrosis. Recovery of the zone of stasis would require restored perfusion and neoangiogenesis to reestablish blood flow to this zone to limit ischemic damage.

Unlike other modalities to treat burn wounds, LED therapy, by stimulating cell proliferation and growth factor production would potentially restore perfusion by increasing angiogenesis. Increased angiogenesis would likely result in accelerated healing of the burn wound.

### **CENTRAL HYPOTHESES**

1) LED photostimulation will improve burn wound healing by inducing macrophage proliferation and secretion of pro-angiogenic factors.

2) Increased macrophage proliferation and secretory function will lead to increased angiogenesis in the zone of stasis.

### **SPECIFIC AIMS**

To test these hypotheses, the following specific aims were undertaken.

- a. To measure the effect of different LED wavelengths on burn wound healing. Each of the wavelengths previously used in wound healing studies has the potential to improve burn wound healing, however, many of these studies failed to compare the different wavelengths, often relying only on one or two wavelengths.
- b. To determine the relationship of the angiogenic factors and inflammatory mediators in burn wounds treated with LEDs. Numerous wound healing studies in other models have

demonstrated interactions between NO and VEGF and NO and COX-2 as essential in wound closure; however, their role in burn wound healing is not clear.

- c. To determine if LED photostimulation induces macrophage production of pro-angiogenic factors. Macrophages are central to normal wound healing and activation of macrophages to produce growth factors and other mediators important to the proliferative phase of wound healing would be necessary.

## **CHAPTER 5: MATERIALS AND METHODS**

### **STUDY TYPE AND DESIGN**

#### **In Vitro Model**

A prospective randomized trial in an in vitro model of inflammation.

#### **Animal Model**

A prospective randomized partially blinded trial in a thermal injury rodent model of limited surface area.

### **CELL CULTURE**

#### **Rationale**

The macrophage-like cell line RAW 264.7 (ATCC, Manassas, VA) was chosen because of its ease of growth and its ability to make large amounts of nitric oxide (NO), which was one of the inflammatory mediators of interest. This cell line was established from murine tumors induced with Abelson leukemia virus and express properties of stimulated macrophages (Raschke 1978), such as pinocytosis of neutral red, phagocytosis of zymosan and latex beads, antibody-dependent killing and phagocytosis of sheep erythrocytes, and secretion of lysozyme (Raschke 1978). These cells also make large amounts of NO in response to stimuli, such as lipopolysaccharide (LPS) and interferon- $\gamma$  (IFN- $\gamma$ ). The use of either LPS or IFN- $\gamma$  alone results in markedly elevated levels of NO, however, stimulation with the combination of both LPS and IFN- $\gamma$  results in a much greater increase in nitric oxide production than that seen with either LPS or IFN- $\gamma$  alone (Lorsbach, 1993). The cells were stimulated with LPS and IFN to serve as a positive control, since these factors are known to stimulate NO production.

#### **Cell treatment**

RAW 264.7 cells were grown to confluence in high glucose (4.5 g/dl D-glucose) DMEM (Gibco, Carlsbad, CA), 10% FBS (Gibco), 100 Units penicillin, 100  $\mu$ g streptomycin, and 0.25

$\mu\text{g}$  amphotericin B (antibiotic-antimycotic, Gibco, Carlsbad, CA) at  $37^{\circ}\text{C}$ ,  $10\%$   $\text{CO}_2$  and then plated in triplicate in 24 well plates (Corning, Acton, MA) at a concentration of  $5 \times 10^5$  cells/ml and in 96 well plates (Corning, Acton, MA) (proliferation assays) at the same cell density. Twenty-four hours later, the media was changed to serum-free, phenol-free DMEM. After twenty-four hours of acclimation to serum-free media, cells were either stimulated with or without LPS ( $10 \text{ ng/mL}$ ) (Sigma-Aldrich, St. Louis, MO) and mouse recombinant INF- $\gamma$  ( $100 \text{ U/mL}$ ) (Calbiochem, San Diego, CA). Each experiment was performed in triplicate and was repeated 3 times.

Twenty-four hours following addition of LPS/IFN, both the stimulated and the nonstimulated cells were divided into five groups and underwent LED treatment at the following wavelengths.

- A) Control – no LED
- B)  $670 \text{ nm}$  ( $4 \text{ J/cm}^2$ )
- C)  $730 \text{ nm}$  ( $4 \text{ J/cm}^2$ )
- D)  $880 \text{ nm}$  ( $4 \text{ J/cm}^2$ )
- E) Combination ( $880 \text{ nm}/730 \text{ nm}/670 \text{ nm}$ ) ( $12 \text{ J/cm}^2$ )

Twenty-four hours after LED therapy, conditioned media (cell culture supernatant) was harvested and stored at  $-70^{\circ}\text{C}$ .

## **BURN WOUND ANIMAL MODEL**

### **Rationale**

The inflammatory response to burn injury is more profound than with any other form of trauma. Burns larger than  $40\%$  TBSA exhibit an inflammatory response that involves the whole body. Large thermal burns are associated with systemic effects resulting in elevated nitrite levels and peroxynitrite levels even in unburned skin (Oliveira, 2004). Since the intent of our study was

to focus on the burn wound itself and not on the systemic effects of massive burn injury, we utilized a small animal model of limited burn size (<10% TBSA).

### **Animals and Environment**

Male Sprague Dawley rats (Harlan, Indianapolis, IN) weighing 250 - 300 grams were used throughout the study. The rats were acclimated in a vivarium for one week prior to beginning the experiment. The rats were housed in groups of 2 - 3 per cage prior to the experiment to allow for socialization. Following the procedure, the animals were housed in separate steel micro-isolators in order to prevent cross infection of wounds, interference, and debridement of burn wounds by cohabitating animals and to facilitate correct LED photostimulation administration to the animals. Food and water were allowed ad libitum. Food and water containers were situated such that they were easily accessible to injured animals recovering from anesthesia associated with burning. The climate in the vivarium was monitored and temperature controlled within the range of 68-73°C, and humidity within the range of 55-60%.

All standard principles of care were followed and approval for the animal protocol was obtained from the UTMB Institutional Animal Care and Use Committee.

### **Anesthesia and Analgesia**

Anesthesia was induced by inhalational isoflurane anesthesia for four minutes. The rats were placed in a specially constructed transparent Plexiglass induction chamber connected to an isoflurane vaporizer. Isoflurane was delivered with oxygen for three minutes, at a rate of four liters per minute in order to produce a final mixture containing 2-4% isoflurane. The entire induction chamber apparatus was placed within a standard extraction hood allowing exhaust gases, and gas release caused by operation of the chamber to be safely scavenged. Inhalational anesthesia reduced the procedural stress experienced by the animals during handling and

subsequent burning.

Anesthesia was maintained by immediate intraperitoneal injection of 0.45 ml of an anesthetic mixture of ketamine HCl, 0.3 ml of 100 mg/ml solution, and xylazine HCl, 0.15 ml of 1 mg/ml solution. Buprenorphine (0.1-1.0 mg/kg) was administered for post burn analgesia twice daily as needed.

### **Burn Procedure (Contact Burn Model)**

The dorsum of each animal was shaved and depilated with a commercially available depilatory (NAIR) (Church & Dwight, Inc., Princeton, NJ) according to the manufacturer's instructions. A burn was created by placing the anesthetized rat prone and then placing a customized thermally insulated metal probe (diameter = 3/4 inch) preheated to 100°C, onto the animal's dorsum for 10 seconds to create the contact burn. This was repeated for a total of five dorsal wounds. Total body surface area burned was 8%. A third degree/full thickness burn wound of consistent thickness was created. The rats were allowed to recover on a warming pad and then returned to their isolators when awake and moving on their own. A daily progress report was kept in the vivarium notebook.

### **Euthanasia**

Apathy, loss of body weight greater than 20%, inability to ambulate, feed, or drink was considered signs of distress for the animals. Animals displaying these signs underwent humane euthanasia by CO<sub>2</sub> asphyxiation, and death confirmed by open chest.

### **LED TREATMENT**

The animals were randomized into the following groups:

A) burn only – no LED

B) burn + 670 nm (4J/cm<sup>2</sup>)

C) burn + 730 nm ( $4\text{J}/\text{cm}^2$ )

D) burn + 880 nm ( $4\text{J}/\text{cm}^2$ )

E) burn + Combination (880 nm/730 nm /670 nm) ( $12\text{J}/\text{cm}^2$ )

Starting on postburn day #1, the animals underwent daily LED treatment. The rats were placed individually into specially designed plexiglass cages and the LED light sources were placed one centimeter from the animal's dorsum.

## **LIGHT SOURCES**

SpectraLife Solid State Light Sources (Quantum Devices, Inc., Barneveld, WI), are monolithic arrays of hybrid GaAlAs light emitting diodes designed to emit diffused monochromatic light (Figure 1). The chips have been custom fabricated to emit specific peak wavelengths of photon energy at 670 nm, 730 nm, and 880 nm with bandwidth of 25-30 nm at 50% power, power intensity  $50\text{mW}/\text{cm}^2$  and energy density  $4\text{J}/\text{cm}^2$  when applied for 64 seconds, 55 seconds, and 87 seconds for 670 nm, 730 nm, 880 nm, respectively. Energy output was calibrated using the Model LM2 Silicon Photodetector light sensor with the Fieldmaster readout unit (Coherent, Inc., Palo Alto, CA).

## **SACRIFICE**

The animals were euthanized by CO<sub>2</sub> asphyxiation on post-burn days 3 (n=9/group), 7 (n=9/group), 14 (n=3/group), and 21 (n=1/group). Death was confirmed by open chest.

## **PLANIMETRY**

Following sacrifice, the wounds were traced for surface area measurements and then harvested. Changes in surface area were determined using digital planimetry (SigmaScan, SPSS, Inc., Chicago, IL).

## **BURN WOUND ZONE ENRICHMENT**

Wounds #1 - 3 (Illustration 6) were sectioned into concentric rings of 6 mm, 13 mm, and 19 mm in an attempt to enrich for the different burn wound zones: zone of coagulation, zone of stasis, and zone of hyperemia, respectively. The wound tissue was snap-frozen in liquid nitrogen and stored at -70°C.

The remaining wounds were divided as outlined in the schemata shown in Illustration 6.

## **TENSIOMETRY**

Wound #4 was cut into longitudinal strips with the wound in the center of the strip and then placed on ice prior to immediate tensile strength measurements. The width and thickness of each strip was measured. The strips were pulled to failure using an Instron Materials Testing device, Model 4201 (Instron Corp, Canton, MA), with a 50 Newton (N) load cell at a crosshead speed of 10 cm/min.

## **TISSUE HOMOGENIZATION**

Wound tissue (wounds #1 - 2) previously snap frozen and stored at -70°C was homogenized in tissue lysis buffer (10 mM Tris, pH 7.4, 150 mM NaCl, 1% Triton). Following centrifugation at 14000 rpm for 20 minutes, the supernatant was removed and stored at -70°C.

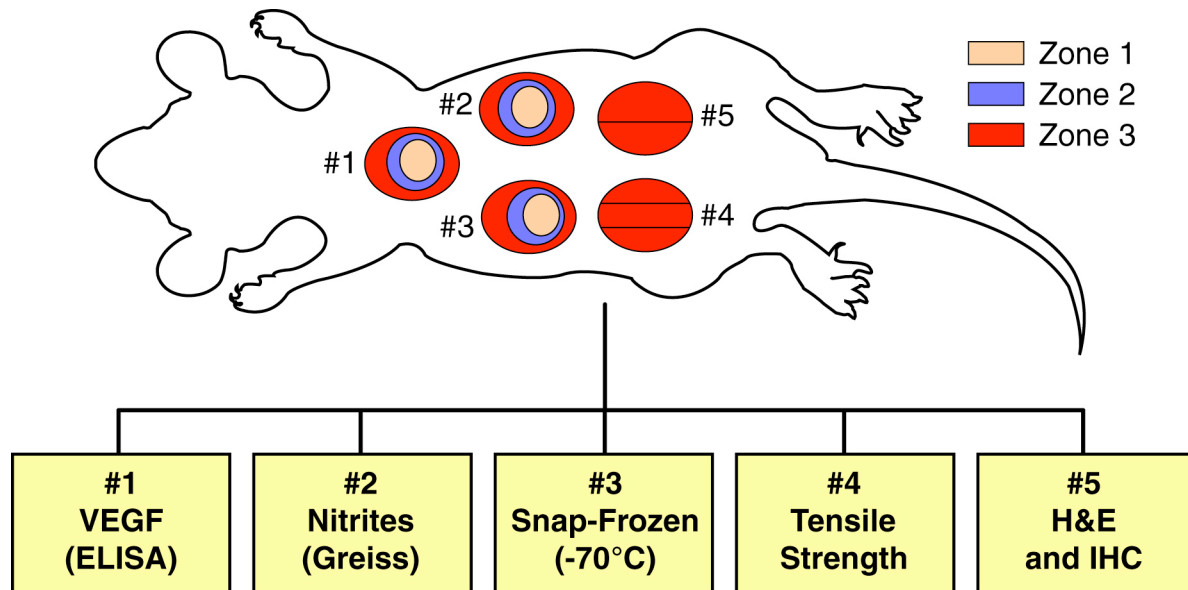


ILLUSTRATION 6: Schemata of rat burn model

## **VEGF ANALYSIS**

VEGF levels were determined using a commercially available ELISA (R&D Systems, Minneapolis, MN) according to the manufacturer's instructions. Briefly, samples from tissue homogenates were diluted (1:5) with calibrator diluent as per manufacturer's instructions and then loaded onto 96 well plates. Recombinant mouse VEGF was used to create the standard curve. Following addition of the conjugate and substrates, the reaction was stopped with the stop solution and the optical density was read on a Bio-Tek EL800 microplate reader (Bio-Tek Instruments, Inc., Winooski, VT) at 450 nm. Protein levels in the tissue homogenates were determined using a commercially available kit according to the BCA (bicinchoninic acid) method (Pierce Biotechnology, Rockford, IL). VEGF levels were expressed as picograms per milligram protein.

Samples from macrophage-conditioned media underwent similar processing with the exception of dilution to 1:4 with calibrator diluent.

## **NITRITE ANALYSIS (GREISS REACTION)**

Nitrite levels, an index of nitric oxide synthesis, were determined using the Greiss reaction as described by Schaffer et al (Schaffer 2004). Although both nitrites ( $\text{NO}_2$ ) and nitrates ( $\text{NO}_3$ ) are end products of nitric oxide synthesis, the Greiss assay measures nitrites. In order to measure the total accumulated NO oxidation products, nitrate must be reduced to nitrite with NADH-dependent nitrate reductase (Tarpey 2001) followed by removal of NADH prior to spectrophotometric detection of nitrites by the Greiss reaction. Although the Greiss assay measures only nitrites, it is a simple, reliable, and reproducible technique (Schaffer 2004) that is widely accepted to indirectly measured nitric oxide levels.

The Greiss reaction is a diazotization reaction that was originally described by Greiss in

1879. Briefly, samples were diluted (1:5) with 1xPBS and then loaded onto 96 well plates. Sodium nitrite was used to create the standard curve. Fifty microliters of Greiss reagent (1% sulfanilamide, 0.1% naphthyethylenediamine dihydrochloride in 5% phosphoric acid) (Sigma-Aldrich, St. Louis, MO) was added to 50  $\mu$ l of diluted sample and incubated for 10 minutes in the dark. The optical density was read on a Bio-Tek EL800 microplate reader at 540 nm. Nitrite levels were expressed as micromoles/microgram sample.

### **MACROPHAGE PROLIFERATION**

Cellular proliferation was assessed using BrdU incorporation according to the manufacturer's instructions (Cell Proliferation Biotrak ELISA System, Amersham Biosciences, Piscataway, NJ). After conditioned media was harvested, the cells were labeled with BrdU for 2 hours. The labeling medium was removed and the cells were incubated in fixative solution for 30 minutes at room temperature. The fixative was then removed and blocking reagent added. Following 30-minute incubation, the blocking buffer was removed and peroxidase-labeled anti-BrdU added for 30 minutes at room temperature. Following washing and substrate addition, the optical density was measured on a Bio-Tek EL800 microplate reader at 450 nm.

### **LIGHT MICROSCOPY**

A 3 mm wide strip was excised from the center of wound #5 and embedded in paraffin following overnight fixation in 10% neutral buffered formalin (Sigma-Aldrich, St. Louis, MO). 3  $\mu$ m sections were created for hematoxylin and eosin staining and immunohistochemistry. H & E staining was analyzed semiquantitatively. The slides were scored for reepithelialization, granulation tissue formation, collagen content, hair follicle number and cellular infiltration (26) of fibroblasts, macrophages, and polymorphonuclear neutrophils (PMNs). Slides were randomized, evaluated under 10x magnification and scored

with the aid of a masked pathologist unaware of the treatment groups, and given values ranging from 0-4 in each category, with 0 being none and 4 being many.

This method creates a numerical value for each histologic criterion, which can then be presented as the mean, standard deviation (SD), and standard error of the mean (SEM) for each test group.

## **IMMUNOHISTOCHEMISTRY**

Endogenous peroxidases were blocked by incubation with 1% H<sub>2</sub>O<sub>2</sub>, and nonspecific binding was blocked with diluted serum of the animal of origin of the primary antibody. Sections were incubated overnight with diluted primary antibody at 4°C. Following washing steps, the slides were incubated with secondary antibodies specific for the animal of origin of the primary antibody and a streptavidin-horseradish peroxidase complex (Vectastain Elite ABC Kits, Vector Laboratories, Burlingame, CA), followed by DAB (3, 3'-diaminobenzidine) (Biocare Medical, Walnut Creek, CA) and counterstaining with hematoxylin (Richard Allen Scientific, Kalamazoo, MN). Commercially available antibodies for VEGF (1/500 dilution) (Rabbit polyclonal, Biogenex, San Ramon, CA), iNOS (1/100 dilution) (Mouse monoclonal, Transduction Laboratories, BD Biosciences, San Diego, CA), COX-2 (1/1000 dilution) (rabbit polyclonal, Cayman Chemical, Ann Arbor, MI), Factor VIII (1/1000) (rabbit polyclonal, DAKOCytomation, Carpinteria, CA), and ED-1 (1/100 dilution) (mouse monoclonal, Serotec, Raleigh, NC) were used. Normal unburned rat skin was used as a control. Slides were dehydrated, mounted, and viewed to determine qualitative and quantitative changes between the different treatment groups for VEGF, iNOS, Factor VIII, and COX-2. Slides stained for ED-1 (rat macrophage marker) were analyzed qualitatively to determine whether macrophages were responsible for the changes seen in iNOS, VEGF, and COX-2.

The Image Pro Plus V. 4.5 (Media Cybernetics, Atlanta, GA) analysis program was used to quantify the area of DAB positive staining per high-powered field (HPF) in each wound section. The program calculates the area comprised of pixels having intensity values within the selected range is reported.

For iNOS, VEGF, and COX-2 immunohistochemistry, data are expressed as Area ( $\mu\text{m}^2$ )/HPF. For Factor VIII immunohistochemistry, the number of Factor VIII+ blood vessels was assessed by manually counting the number of DAB+ luminal structures containing red blood cells.

#### **DATA ANALYSIS**

A one-way analysis of variance with post-hoc comparisons using Tukey's test was used to determine the statistical significance between groups (GraphPad Prism v4.06, GraphPad, San Diego, CA). A p-value of less than 0.05 was considered significant. Data are presented as mean  $\pm$  SEM.

## CHAPTER 6: RESULTS

### PLANIMETRY

Longer wavelengths appeared to decrease wound surface area. Wound surface area decreased 25% and 50% in the 880 nm and combination treated groups, respectively, compared to control (Figure 2).

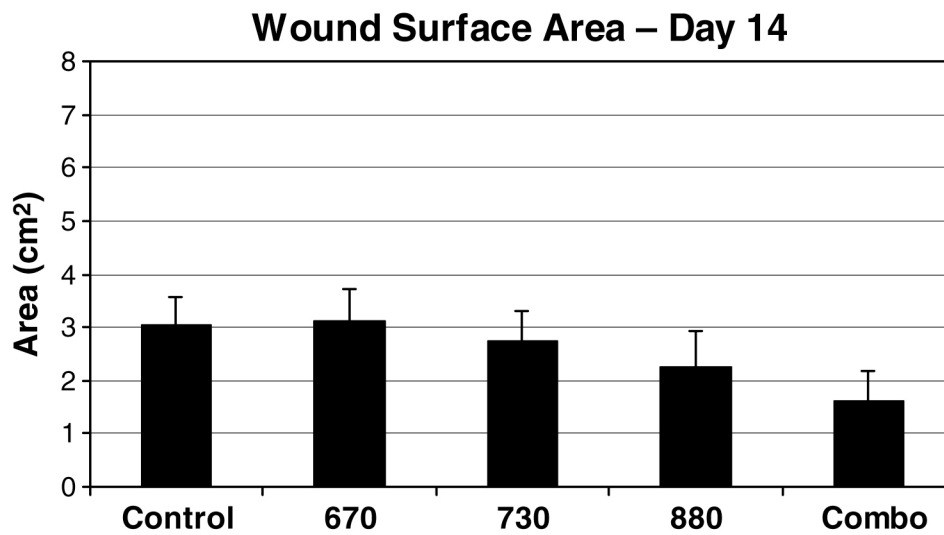


FIGURE 2: Wound surface area on postburn day 14. Combination (combo) LED-treated wounds were approximately 1 cm<sup>2</sup> smaller than wounds of other groups. N=3 per treatment group.

## TENSIOMETRY

Tensile strength was not statistically significantly affected by LED therapy at any wavelength or any time point (Figure 3).

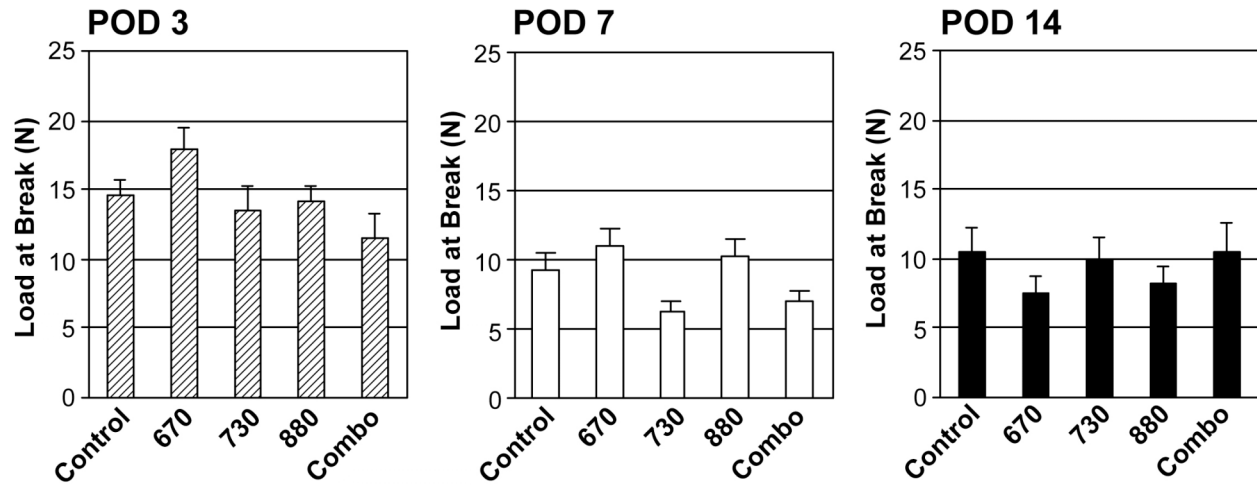


FIGURE 3: Tensiometry at postburn day 3, 7, and 14. N=3 per treatment group.

## VEGF LEVELS

Initial experiments were performed to determine the kinetics of VEGF production. Compared to postburn days 3 and 14, VEGF levels were increased at postburn day 7 in whole wound homogenates from control (no LED) animals (Figure 4).

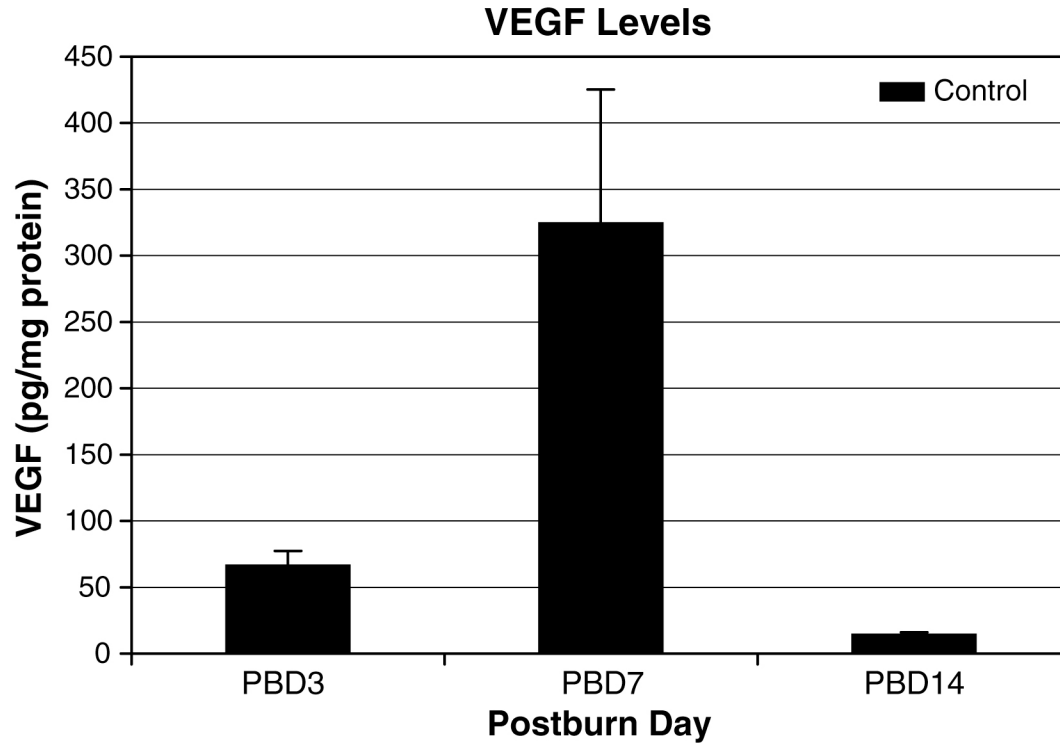


FIGURE 4: VEGF levels at postburn days 3, 7, and 14 in whole wound homogenates compared to control (no LED) rats. N=3 per treatment group.

## NITRITE LEVELS

Similarly, initial experiments were performed to determine kinetics of nitrite production.

Nitrite levels were greatest at postburn days 3 and 7 with decreasing levels by postburn day14

(Figure 5).

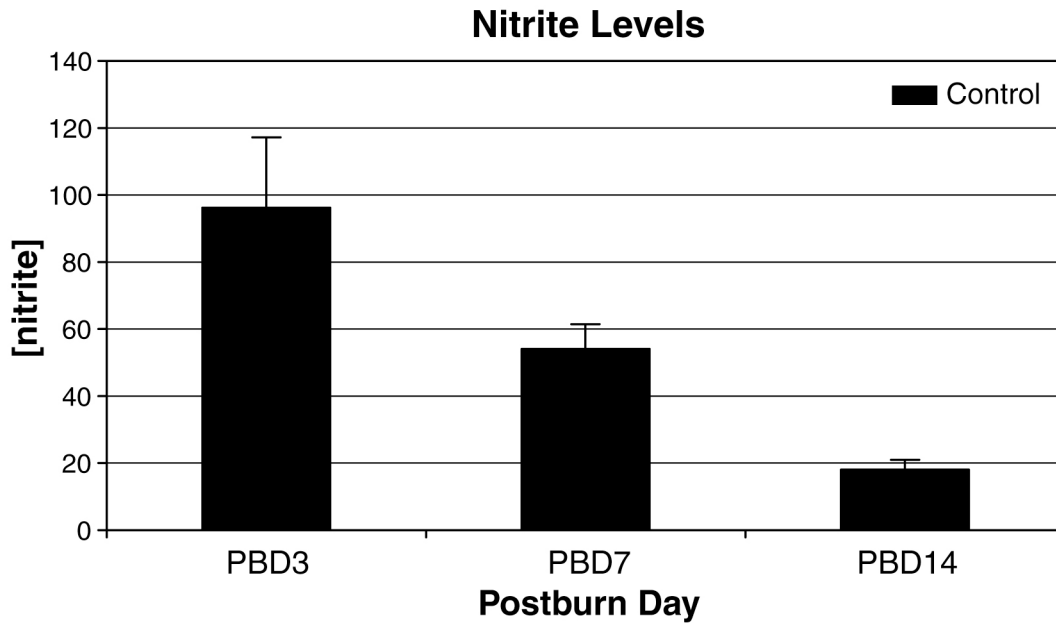


FIGURE 5: Nitrite levels at postburn days 3, 7, and 14 in whole wound homogenates compared to control (no LED) rats. N=3 per treatment group.

## LIGHT MICROSCOPY

Reepithelialization increased 25% in the 730 nm group (730 nm:  $x = 1.11 \pm 0.20$ ,  $n = 9$ ; control:  $x = 0.89 \pm 0.20$ ,  $n = 9$ ). This finding was associated with a decrease of 23% in macrophage number in the 730 nm group (730 nm:  $x = 1.11 \pm 0.11$ ,  $n = 9$ ; control:  $x = 1.44 \pm 0.18$ ,  $n = 9$ ).

Collagen content increased 45% compared to control in the 880 nm group (880 nm:  $x = 1.30 \pm 0.37$ ,  $n = 9$ ; control:  $x = 0.89 \pm 0.35$ ,  $n = 9$ ). Yet, in the 880 nm group, there was a 23% decrease in the fibroblast number (880 nm:  $x = 1.20 \pm 0.13$ ,  $n = 9$ ; control:  $x = 1.55 \pm 0.29$ ,  $n = 9$ ).

Longer wavelengths and higher energy fluences incrementally decreased granulation tissue with combination having 33% less granulation tissue compared to the control group (combination:  $x = 1.33 \pm 0.24$ ,  $n = 9$ ; control:  $x = 1.78 \pm 0.22$ ,  $n = 9$ ).

Qualitatively, there appeared to be increased numbers of viable hair follicles. This was confirmed by the semiquantitative scoring which showed that the 730 nm, 880 nm and combination groups had 33%, 50% and 26% more hair follicles compared to the control group, respectively (730 nm:  $x = 2.22 \pm 0.70$ ,  $n = 9$ ; 880 nm:  $x = 2.50 \pm 0.58$ ,  $n = 9$ ; combination:  $x = 2.11 \pm 0.68$ ,  $n = 9$ ; control:  $x = 1.67 \pm 0.67$ ,  $n = 9$ ).

## **IMMUNOHISTOCHEMISTRY**

### **iNOS**

The iNOS antibody (seen in brown) localizes to the inflammatory cell layer just below the necrotic epidermis and appears to localize most intensely to macrophage-like cells (Figure 6A). iNOS positive area was greatest in the postburn day 7 animals, particularly in the control and combination groups, with decreased levels in the remaining treatment groups (combination:  $x = 39930 \pm 12310 \mu\text{m}^2$ ,  $n = 9$ ; control:  $x = 25810 \pm 11613 \mu\text{m}^2$ ,  $n = 9$ ) (Figure 6B).

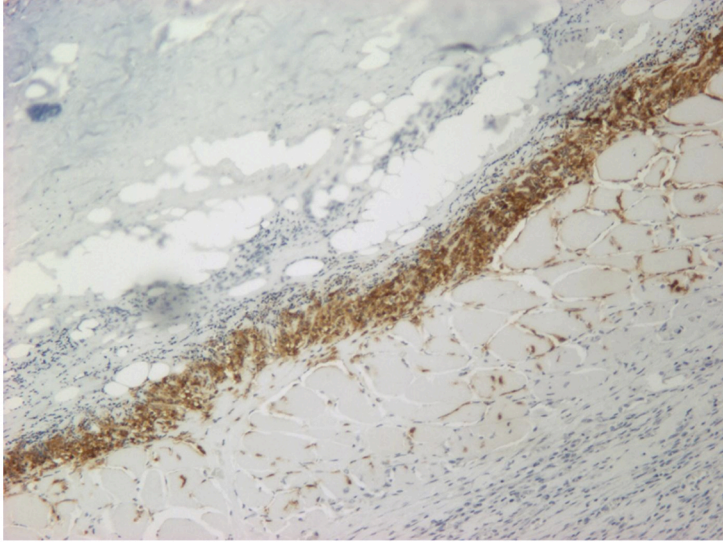
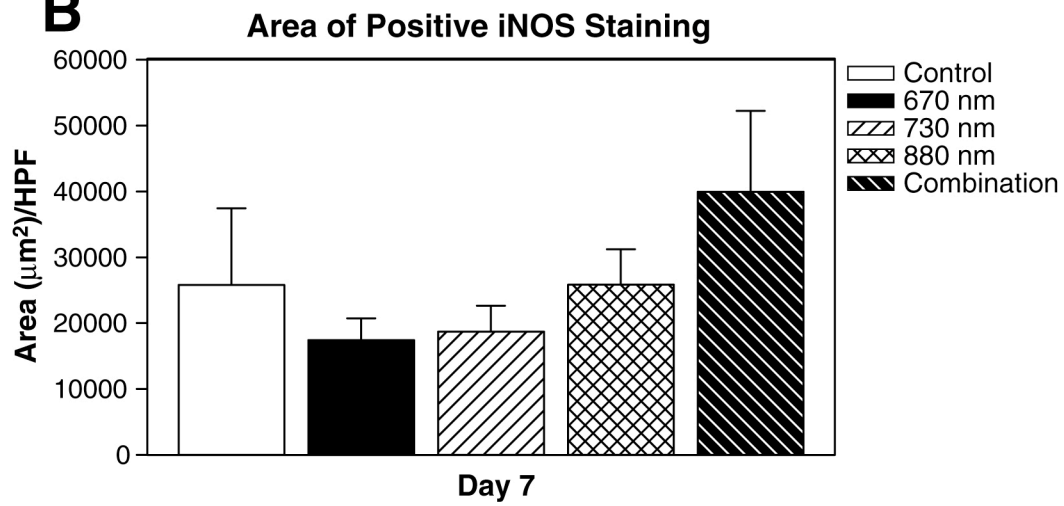
**A****B**

FIGURE 6: iNOS immunohistochemistry. A) iNOS antibody localized to the inflammatory cell layer in the burn wound. B) iNOS positive area in postburn day 7 burn wounds. N=9 per treatment group.

## VEGF

VEGF protein was expressed by normal and burned tissue, although the amount of staining appeared to be greater in the wound bed. In normal skin, hair follicles and the epithelial cell layer were VEGF positive. In the burn wound, VEGF localized to macrophage-like cells in the inflammatory cell layer as well as to fibroblast-like and macrophage-like cells in the dermis and below the nonviable panniculus (Figure 7A). The VEGF positive area was greater at day 7, and there is an apparent increase in VEGF levels in the combination group (combination:  $x = 29571 \pm 2779 \mu\text{m}^2$ ,  $n = 6$ ; control:  $x = 22070 \pm 2115 \mu\text{m}^2$ ,  $n = 6$ ) (Figure 7B).

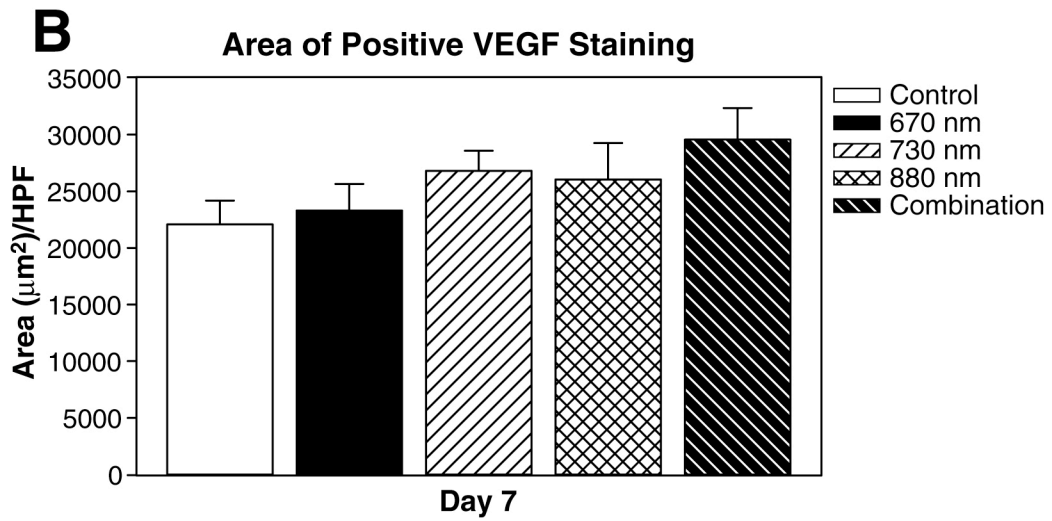
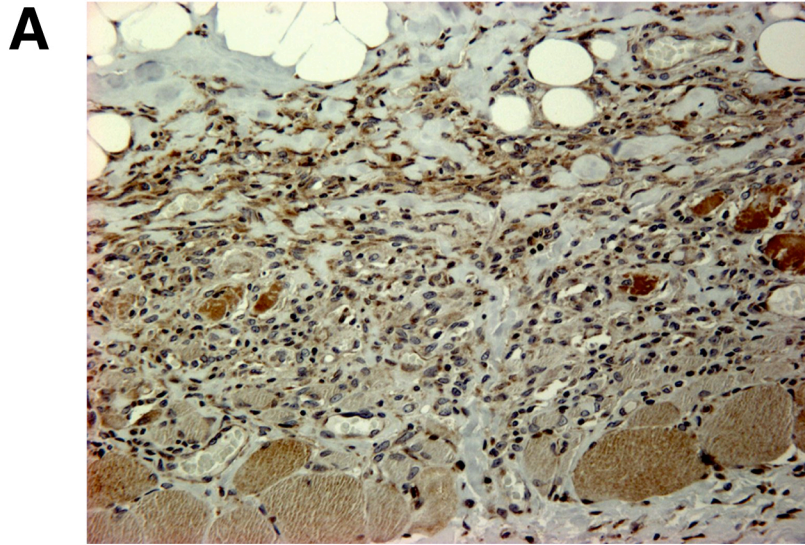


FIGURE 7: VEGF immunohistochemistry. A) VEGF antibody localized to macrophage-like cells in the burn wound. B) VEGF positive area in postburn day 7 burn wounds. N= 6 per treatment group.

### **Factor VIII**

The number of Factor VIII positive blood vessels was assessed by manually counting the number of DAB stained luminal structures containing red blood cells (Figure 8A). Blood vessel number was greatest at day 7 with statistically significantly increased numbers of blood vessels per HPF in the combination group compared to control (combination:  $x = 16.01 \pm 1.26$ ,  $n = 9$ ; control:  $x = 11.89 \pm 0.80$ ,  $n = 9$ ) ( $p < 0.05$ ) (Figure 8B).

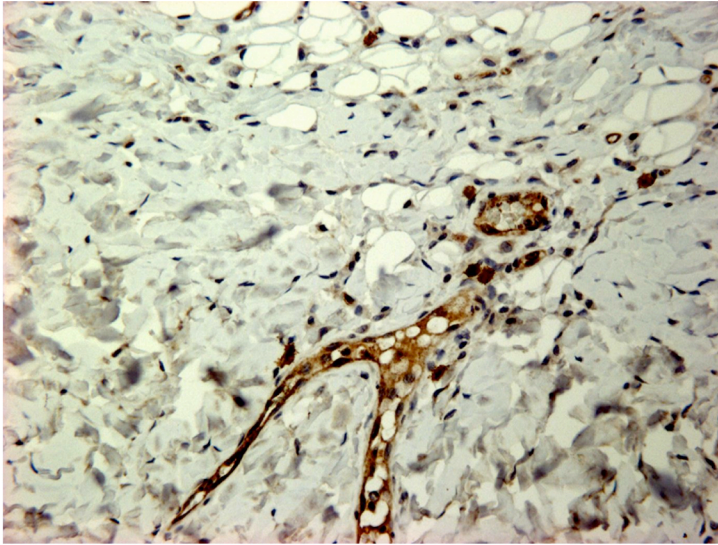
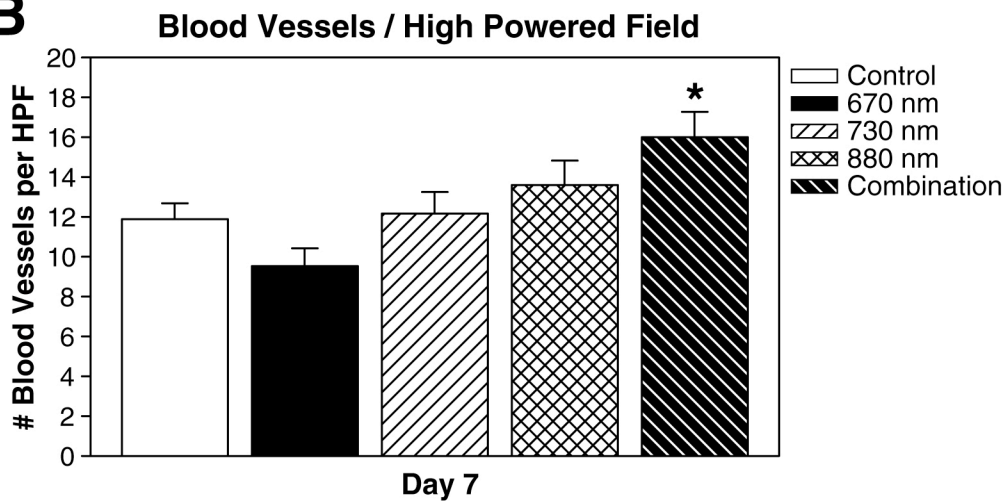
**A****B**

FIGURE 8: Factor VIII immunohistochemistry. A) Factor VIII antibody localized to luminal structures containing red blood cells. B) Factor VIII positive blood vessels in postburn day 7 burn wounds. N=9 per treatment group. \*  $p < 0.05$  combination treatment compared to control (no LED).

## COX-2

In the burn wound, COX-2 is low at post burn day (PBD) three ( $x = 222 \pm 201 \mu\text{m}^2$ ,  $n = 6$ ) peaks at PBD seven ( $x = 56399 \pm 11855 \mu\text{m}^2$ ,  $n = 6$ ), and remains elevated for as long as 21 days (PBD14:  $x = 23028 \pm 10725 \mu\text{m}^2$ ,  $n = 3$ ; PBD 21:  $x = 8444 \pm 7055 \mu\text{m}^2$ ,  $n = 1$ ) in the control group. LED treatment with 670 nm was found to significantly increase the level of COX-2 expression as assessed by immunohistochemistry ( $x = 182094 \pm 51444 \mu\text{m}^2$ ,  $n = 3$ ) at PBD 14 compared to control ( $x = 23028 \pm 10725 \mu\text{m}^2$ ,  $n = 3$ ) ( $p < 0.01$ ) (Figure 9). At PBD 3, 7 and 21, there were no significant differences between the different treatment groups (data not shown).

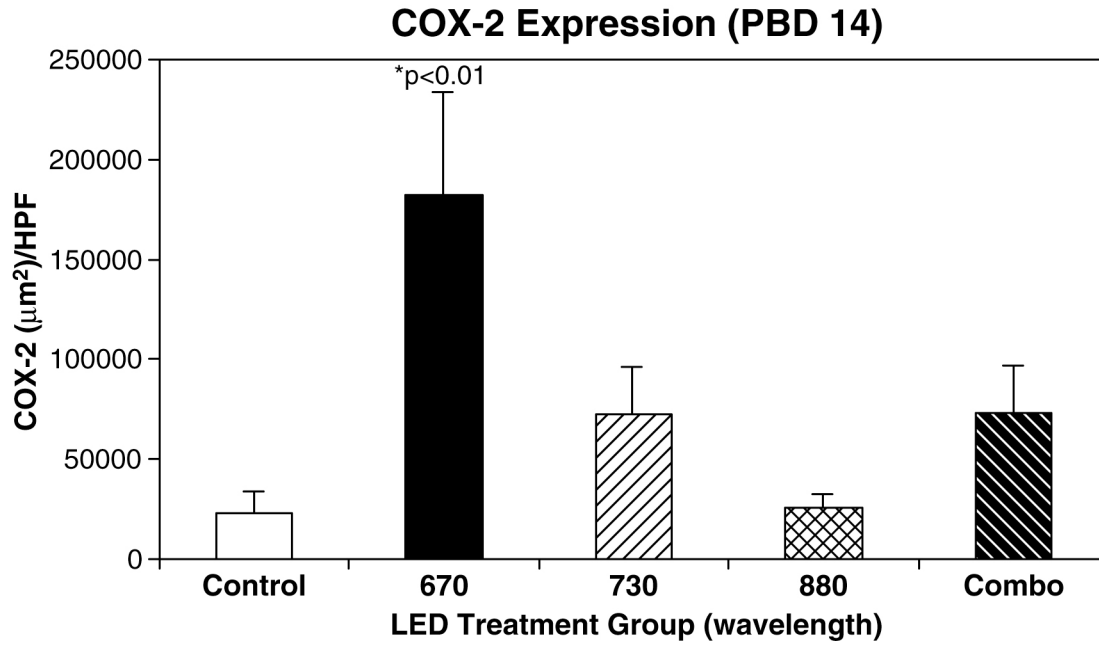


FIGURE 9: COX-2 immunohistochemistry in LED-treated groups. COX-2 expression in postburn day 14 burn wounds. N=3 per treatment group; \* $p < 0.01$  670 nm vs. control (no LED).

**ED-1**

Macrophages appear to be important sources of iNOS, VEGF, and COX-2 in the healing burn wound, as seen by intense DAB localization in macrophage-like cells. This is confirmed with immunohistochemistry using an anti-rat ED-1 antibody (Figures 10A-C). ED-1 is specific to rat macrophages, particularly in tissues, such as spleen and skin. A large number of ED-1+ cells were seen in different portions of the burn wound, particularly in the inflammatory cell layer just below the dermis, and in the deep dermis above the panniculus and in the connective tissue layer just below the panniculus. These cells were also positive for iNOS (Figure 10A), VEGF (Figure 10B), and COX-2 (Figure 10C).

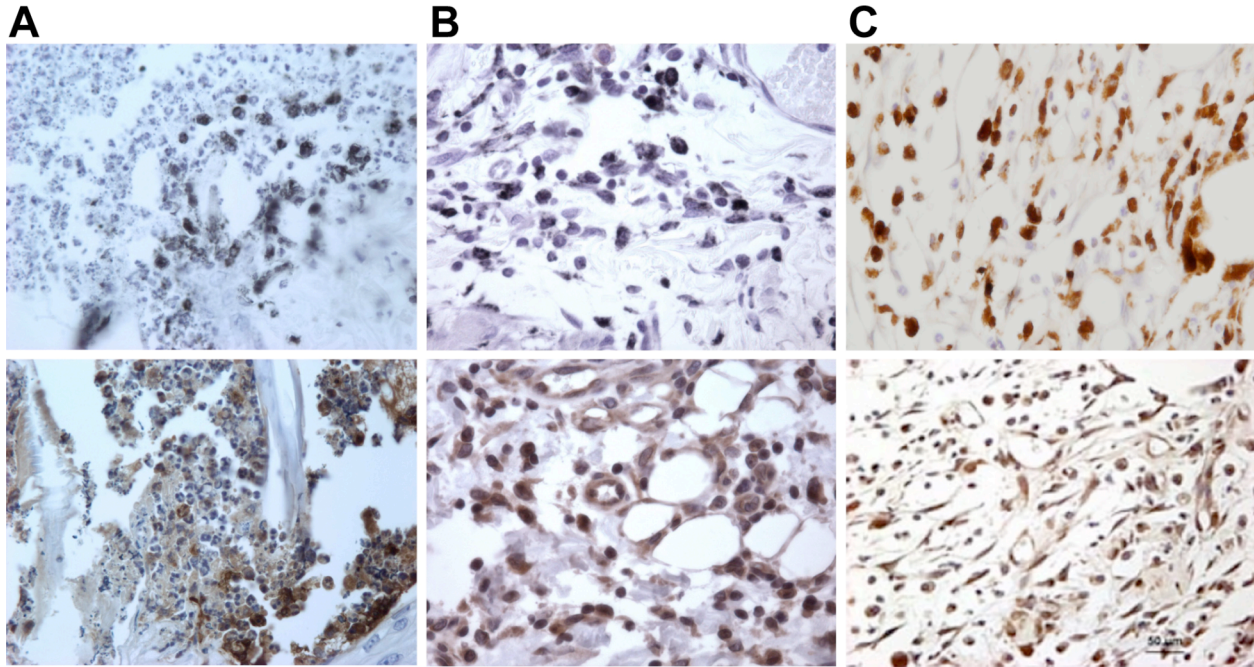


FIGURE 10: A) ED-1 (top left) and iNOS (bottom left) immunohistochemistry (40x magnification). iNOS and ED-1 antibodies localized to macrophages in the burn wound. B) ED-1 (top center) and VEGF (bottom center) immunohistochemistry (40x magnification). VEGF and ED-1 antibodies localized to macrophages in the burn wound. C) ED-1 (top right) and COX-2 (bottom right) immunohistochemistry (40x magnification). COX-2 and ED-1 antibodies localized to macrophages in the burn wound.

## **VEGF AND NITRITE LEVELS IN BURN WOUND ZONES**

### **Burn wound zones**

At days 3 and 7, VEGF levels were increased in the zone of hyperemia compared to the zone of coagulation. Combination therapy resulted in increased VEGF levels in the zone of hyperemia at day 7 (combination:  $x = 235.47 \pm 42.77$ ,  $n = 9$ ; control:  $x = 153.38 \pm 16.89$ ,  $n = 9$ ) (Figure 11A).

Nitrite levels were decreased in the zone of hyperemia and elevated in the zone of coagulation at day 7 (Figure 11B).

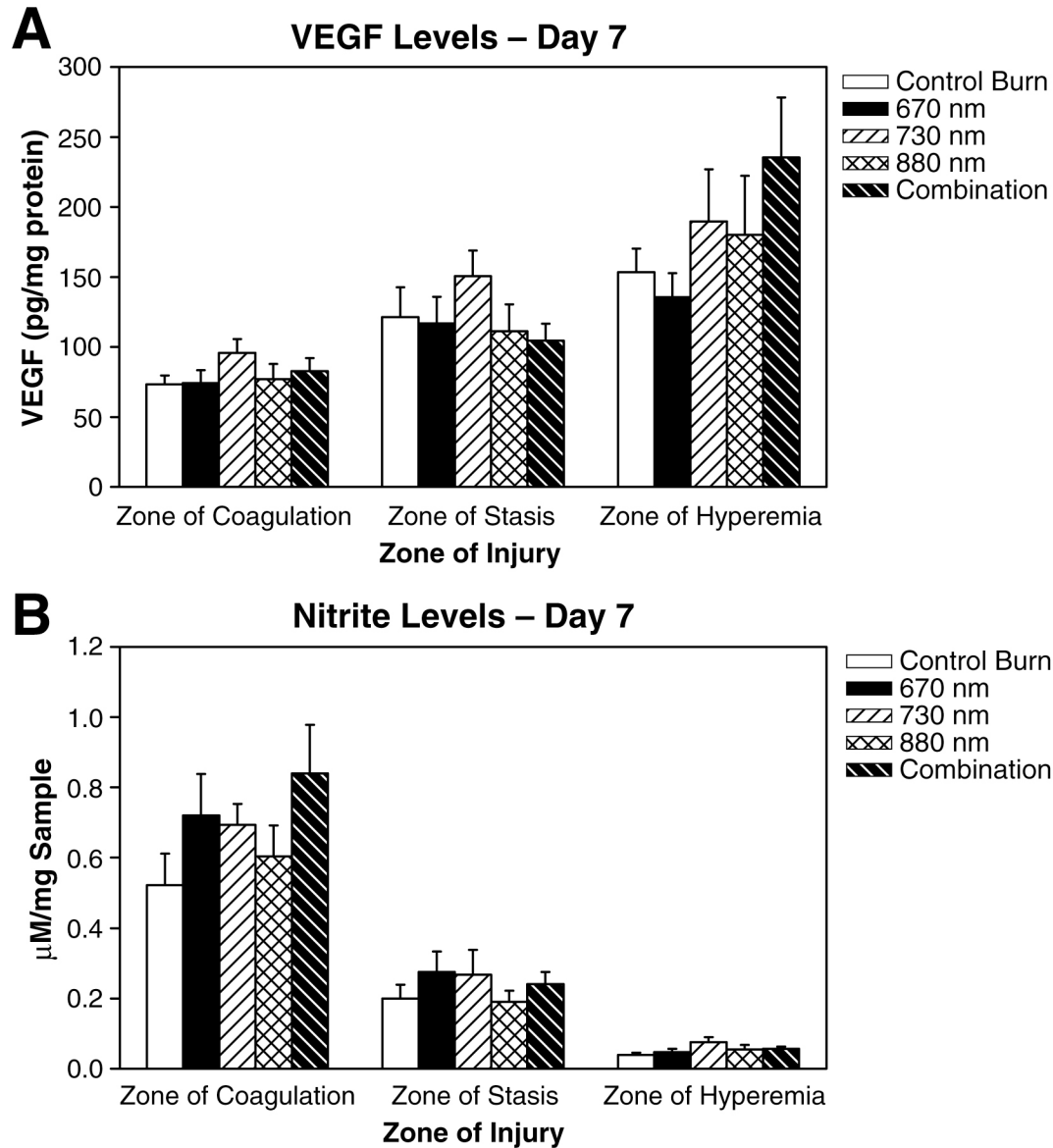


FIGURE 11: Pro-angiogenic factors in the different burn wound zones at postburn day 7. A) VEGF levels B) Nitrite levels.

**SUMMARY OF IMMUNOHISTOCHEMISTRY**

The immunochemistry results are represented in Figure 12.

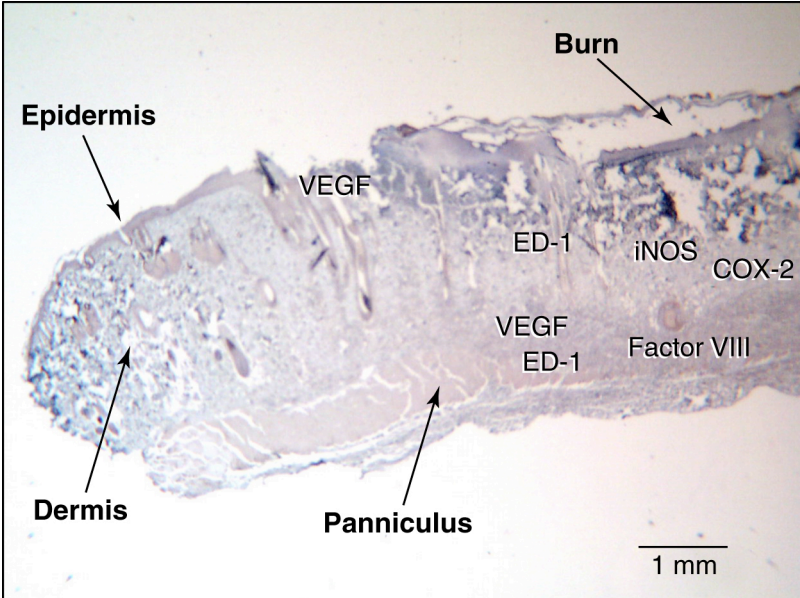


FIGURE 12: Immunohistochemistry summary – rat skin (1x magnification).

## **MACROPHAGE CULTURES**

### **VEGF levels in LED-stimulated macrophage cultures**

VEGF levels were significantly elevated in cultures stimulated by both lipopolysaccharide and interferon (LPS/IFN) compared to nonstimulated groups. There was no statistically significant intergroup differences among the LPS/IFN stimulated groups, although there was an apparent decrease in the VEGF levels in the 730 nm LPS/IFN group.

In the groups that did not receive LPS/IFN, but were treated with LED photostimulation, treatment with an isolated wavelength of 880 nm ( $4\text{J}/\text{cm}^2$ ) and combination therapy ( $12\text{J}/\text{cm}^2$ ) with three wavelengths including 880 nm produced elevated VEGF levels (Figure 13). Combination therapy (880 nm wavelength and greater energy fluence) produced significantly higher VEGF levels compared to control ( $p=0.041$ ). Similar to the LPS/IFN stimulated group, LED treatment with 730 nm also resulted in decreased VEGF by macrophages that had not been stimulated by LPS/IFN.

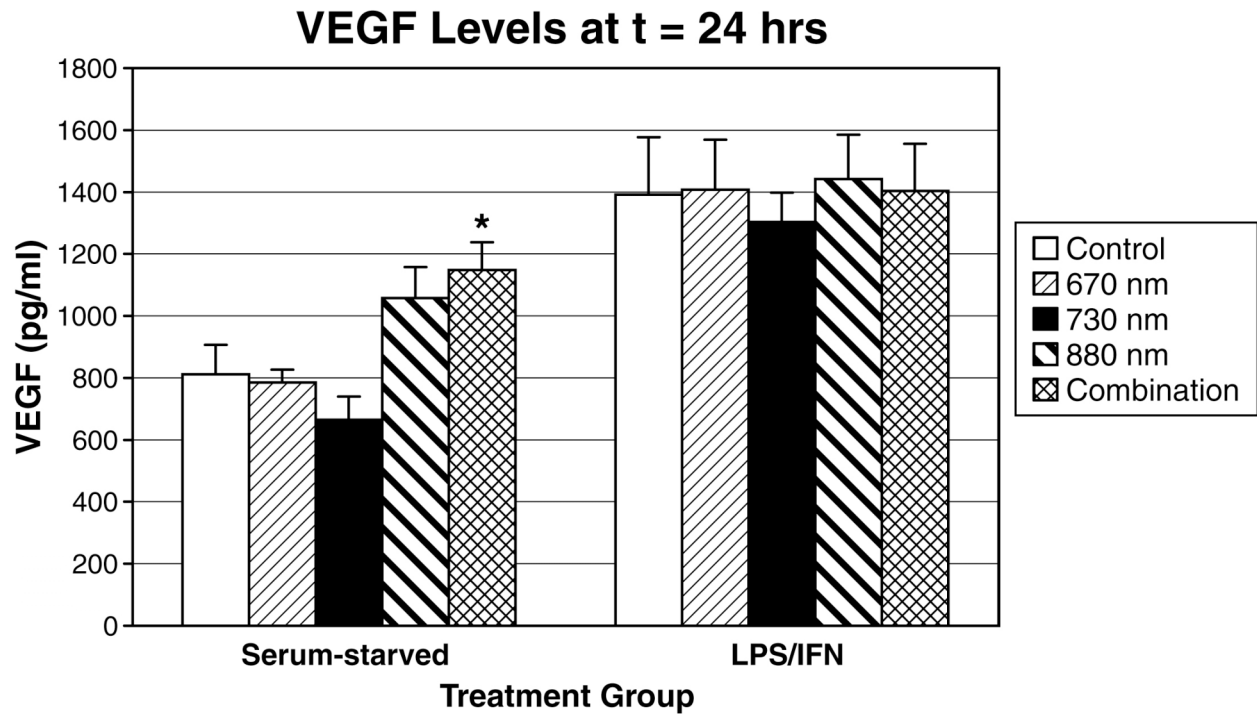


FIGURE 13: Effect of LED treatment on VEGF levels in LPS/IFN stimulated and non-stimulated macrophages. The nonLPS/IFN stimulated (serum-starved) cells are on the left side of the graph and the LPS/IFN stimulated cells on the right side of the graph. (\* $p < 0.05$ , combination versus control in nonLPS/IFN stimulated)  $N = 3$ /treatment. VEGF levels are expressed as mean  $\text{pg/ml} \pm \text{SEM}$

### **Nitrite levels in LED-stimulated macrophage cultures**

Nitrite levels were elevated in the LPS/IFN stimulated groups compared to the nonstimulated groups. There was a statistically significant decrease in the 730 nm treated LPS/IFN stimulated group compared to the all the other groups that received LPS/IFN stimulation (Figure 14).

In the non-LPS/IFN-stimulated groups, nitrites were elevated in the 880 nm and combination-treated groups, while a decrease was noted in the 730 nm treated group (Figure 15). The difference between the 880 nm and combination groups versus the 730 nm treatment group was statistically significant ( $p < 0.05$ ).

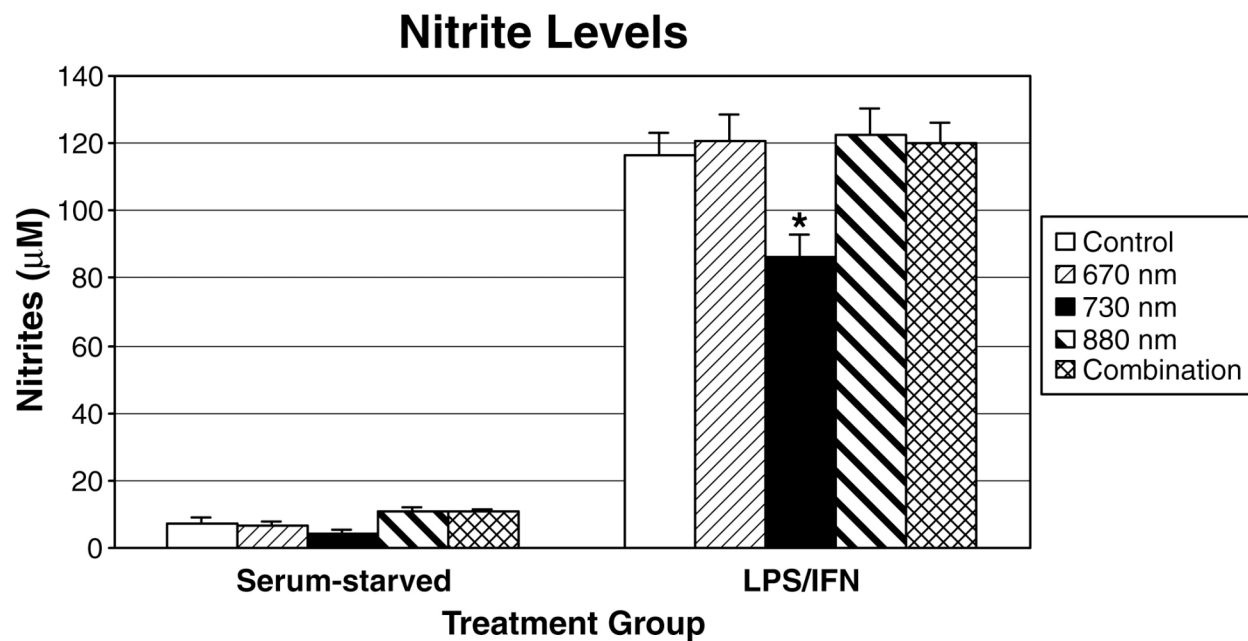


FIGURE 14: Effect of LED treatment on nitrite levels in LPS/IFN stimulated and non-stimulated macrophages. The nonLPS/IFN stimulated (serum-starved) cells are the left side of the graph and the LPS/IFN stimulated cells on the right side of the graph. (\* $p < 0.05$ , 730 nm versus others in LPS/IFN stimulated)  $N=3$ /treatment. Nitrite levels are expressed as mean  $\mu\text{M} \pm \text{SEM}$ .

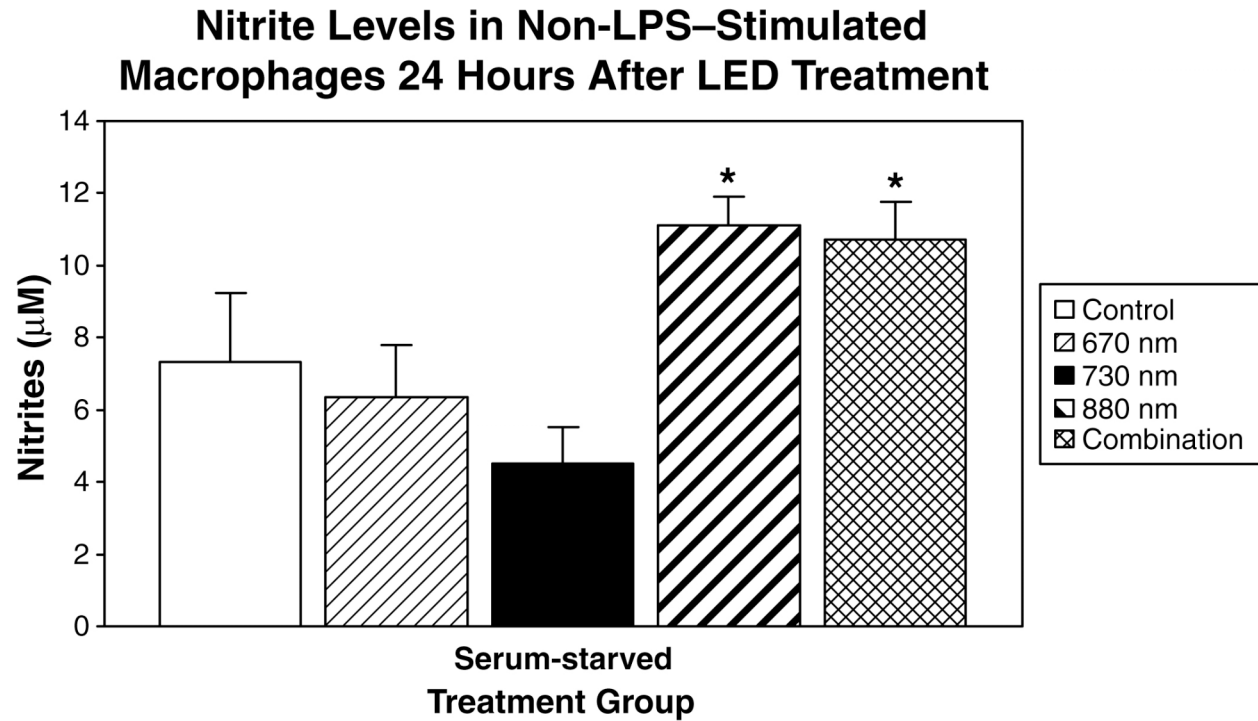


FIGURE 15: Effect of LED treatment on nitrite levels in nonLPS/IFN stimulated macrophages. (\*p<0.05, 880 nm and combination versus 730 nm) N=3/treatment. Nitrite levels are expressed as mean µM ± SEM.

### **Correlation between Nitrite and VEGF level**

A direct positive correlation existed between VEGF and NO levels in conditioned media harvested from LED-treated macrophage cell cultures (Figure 16). The slopes of the lines of best-fit for the different treatments were very different, with the nonstimulated arm having a slope approximately 4 times greater than that in the LPS/IFN stimulated arm. Clarification of this correlation could be accomplished by the addition of either exogenous VEGF or NO.

### Correlation of Nitrite Levels to VEGF Production in the RAW 264.7 Macrophage Cell Line

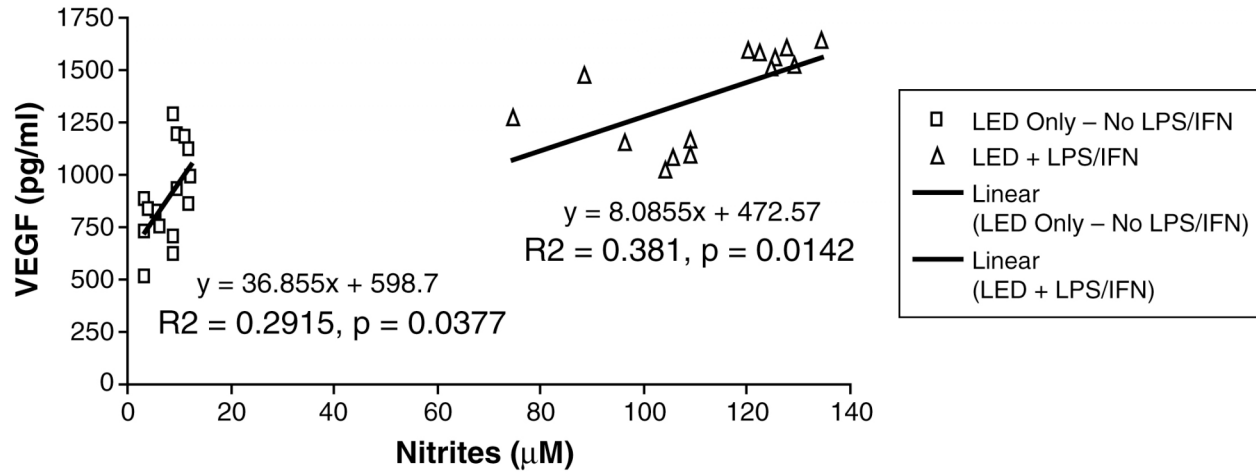


FIGURE 16: Correlation of nitrite levels to VEGF in nonLPS/IFN stimulated and LPS/IFN stimulated macrophages. The left hand set of points represents the nonstimulated cells and the right hand set represents the LPS/IFN stimulated cells. There is a direct positive correlation between nitrites (an indirect measure of NO) and VEGF. The slope of the line for the nonLPS/IFN stimulated cells is four-fold greater than that of the LPS/IFN stimulated cells.

**Macrophage proliferation**

LPS/IFN stimulation resulted in a 25% decrease of macrophage proliferation in all LED-treated groups compared to control ( $p < 0.05$ ) (Figure 17). There was no appreciable difference between the LED-treated groups.

## RAW264.7 Macrophage Proliferation 24 Hours After Treatment with LED

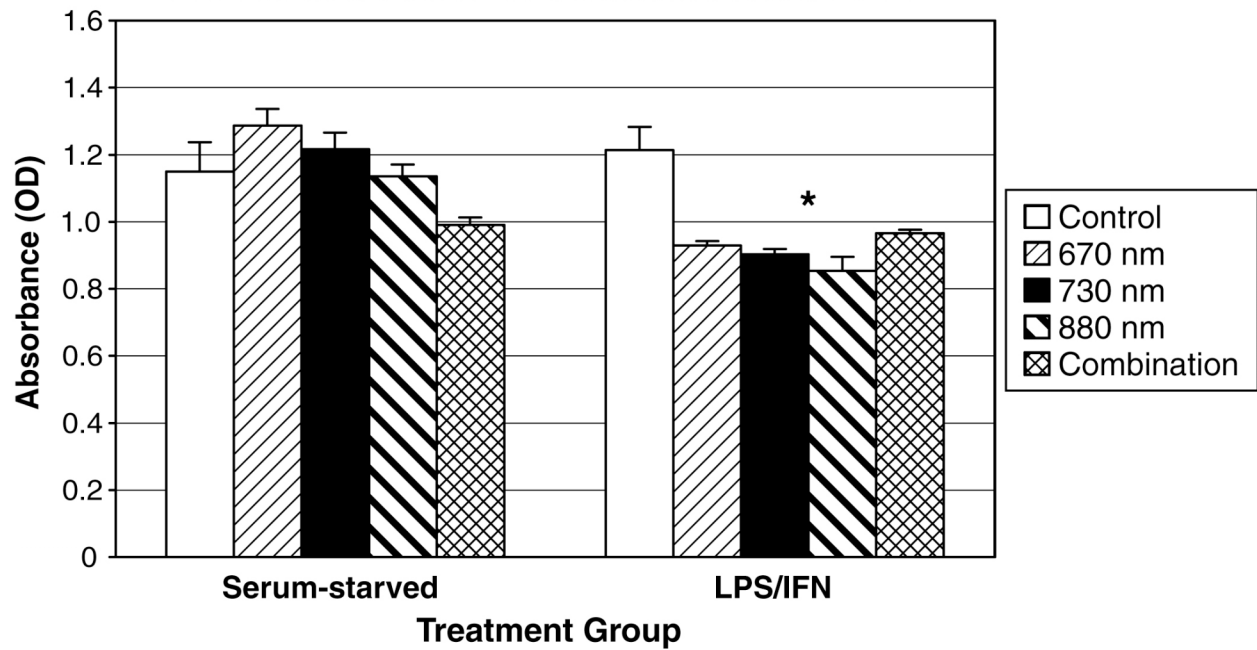


FIGURE 17: Effect of LED treatment on macrophage proliferation in nonLPS/IFN stimulated and LPS/IFN stimulated cells. LPS/IFN stimulation resulted in 25% decrease in macrophage proliferation in all LED-treated groups compared to control (\* $p < 0.05$ , all LED-treatment groups versus control in LPS/IFN stimulated cells)  $N=3$ /treatment group. Proliferation expressed as mean OD  $\pm$  SEM.

## **CHAPTER 7: DISCUSSION**

### **EFFECTS OF LED ON BURN WOUNDS – PREVIOUS STUDIES**

Previous studies have produced conflicting results in burn wounds following LELL or LED therapy. Mester et al. and Rochkind et al. found accelerated healing of burn wounds using ruby (694.3 nm, 0.2J-10J/cm<sup>2</sup> energy densities) and helium-neon (632.8 nm, 10J/cm<sup>2</sup>) (Mester, 1971, Rochkind, 1989). Schlager et al, however, found no beneficial effects of low-power laser light (690 nm and 635 nm) on the healing process of burns in rats (Schlager, 2000). This is corroborated by both Al-Watban and Bayat who, found no beneficial effects of low power lasers on burn wound healing (Al-Watban, 2005, Bayat 2005). These two studies used lasers with wavelengths in the 600 nm range (670 nm and 632.8, respectively).

Unlike previous studies, this investigation used a variety of different wavelengths (670 nm, 730nm, and 880 nm) as well as a combination of the three wavelengths to determine whether LED has any effect on burn wound healing. Interestingly, the 670 nm wavelength and 730 nm wavelengths fared the worst, while combination (880 nm/730 nm/670 nm) and 880 nm had the most beneficial effect on wound healing.

### **TEMPERATURE-INDUCED EFFECTS OF LED**

The mechanism by which LED exerts its effects is not clear, although the possibility of tissue warming has been suggested. Using a diode laser, Stadler et al found that temperature increased with increasing fluences of exposure; however, these increases were very small, leading him to conclude that although potential thermal influences could not be ruled out when examining LELL effects, these thermal effects of irradiation at 830nm could not explain the LELL effect. Our laboratory has also investigated whether LED treatment has a significant thermal effect. Using the Licox microprobe (Harvard apparatus) placed subcutaneously in the rat, we found that the LED treatment did not produce a measurable increase in the temperature of the

rat skin (data not shown), demonstrating that in our model, temperature-induced effects were unlikely. The possibility of an interaction between small temperature-induced effects and the photostimulatory effects produced by LED, however, cannot be completely ruled out.

### **EFFECT OF WAVELENGTH ON WHOLE BURN WOUNDS**

In this study, 880 nm and combination LED photostimulation resulted in elevated numbers of blood vessels per HPF compared to control. The mechanism leading to this new small blood vessel growth is not entirely known, but other studies, including this one, have demonstrated that LED increased levels of VEGF early in the healing period both in vitro and in vivo (Whelan 2000).

Unlike other burn wound studies, which showed no effect in healing after photostimulation (Schlager 2000, Al-Watban 2005, Bayat 2005), our studies showed that the choice of wavelength differentially influences the production of VEGF and nitrites. Furthermore, our investigations demonstrated that higher energy fluences ( $>4\text{J}/\text{cm}^2$ ) were required to have an effect on burn wound healing. Although there was no significant change in tensile strength for any of the LED treatments at any time point, this lack of correlation between angiogenesis and the mechanics of the wound may be secondary to the fact that tensile strength was measured only up to day 14 postburn. The majority of wound healing studies indicate that wound breaking strength only begins to increase after approximately 21 days post-injury (reviewed in Leong, 2004). It is likely the effects of increased angiogenesis may only be seen at later time points.

The in vivo data reported here indicate that both the 880 nm and combination treatments result in the greatest cellular elevations of VEGF and nitrites. Furthermore, 880 nm appears to have additional stimulatory effects on burn wound healing, by increasing collagen deposition (increased collagen content by fewer fibroblasts) and increasing the number of hair follicles, which are sources of stem cells for regenerating epithelium and for wound healing fibroblasts

(Jahoda 2001, Morris 2004). Several factors likely contribute to the success of these particular treatments in this model, in which the burn wounds are covered by a thick burn eschar. One is the depth of penetration of the 880 nm wavelength; studies with low energy lasers have demonstrated that infrared wavelengths, such as 880 nm can penetrate the skin to the hypodermis (Sloney 1980). Secondly, the higher energy fluence in the combination therapy likely allows for penetration of the eschar. The stimulatory effect of the 880 nm wavelength on these full thickness burn wounds is in agreement with a recently published study that demonstrates improved healing of full thickness skin wounds in rats treated with 810 nm diodes (Papillion 2004). Additional treatment groups of repeated doses of a single wavelength for a total of  $12\text{J}/\text{cm}^2$  would allow better delineation of the effect of energy fluence versus wavelength.

Increased angiogenesis in the combination LED group further supports this treatment group as the preferential one to induce small blood vessel growth. This was demonstrated by both increased Factor VIII-positive blood vessels (Figure 8) and VEGF-positive area (Figure 7) in the combination group at day 7. The combination therapy also resulted in increased numbers of hair follicles and elevated levels of iNOS (Figure 6) in the burn wounds, further emphasizing this treatment group as the most optimal LED treatment for this model. It is interesting to note that the finding of increased dermal appendages, such as hair follicles, was also described by DelBeccaro and Robson (DelBeccaro 1980, Robson 1978) and were found to be secondary to improved dermal microcirculation as well. Finally, the combination (880/730/670 nm) LED therapy resulted in a much greater decrease in wound surface area (50%) by day 14 (Figure 2). All these findings suggest that the combination of the three wavelengths may be most beneficial in accelerating healing.

## **EFFECT OF WAVELENGTH ON BURN WOUND ZONES**

Several studies exist that examine the use of agents to prevent burn wound ischemia in attempts to minimize the zone of coagulation and stasis (Battal 1996, Isik 1998), however, this is the first study examining factors important for angiogenesis in the burn wound zones in order to determine whether the zone of stasis could be salvaged and wound size decreased. In this study, VEGF levels were highest in the proposed zone of hyperemia at postburn day 7, with the combination group having the greatest elevations (Figure 11A). Despite our expectations that nitrite levels would be high in this zone of hyperemia and low in the zone of coagulation, our results demonstrate that nitrite levels were actually lowest in the zone of hyperemia and highest in the zone of coagulation at postburn day 7 (Figure 11B). This finding might be explained by the fact that in total wound homogenates from control animals (no LED), nitrite levels peak by postburn day 3 (Figure 5), but decline by postburn day 7. It is likely, therefore, that nitrite levels do not peak in the zone of coagulation until postburn day 7 because of the severity of the burn and the minimal cellular viability present in that zone.

The initial proposed zone of stasis in this series of experiments did not have any appreciable changes in either VEGF or nitrites. This finding suggests that LED photostimulation requires actively metabolizing cells and that there may not have sufficient numbers of active cells. In this study, however, we arbitrarily designated the zones of coagulation, stasis, and hyperemia to be 6 mm, 13 mm, and 19 mm concentric rings of the burn wound. While this method appears rather imprecise, the relative sizes of adjacent zones of injury to one another have never been adequately described in the scientific literature. Classically, the burn wound has been divided into the three discrete zones of injury. Attempts to characterize and to definitively assign a value to the size of one zone of injury in relation to the neighboring zone have, on the whole, been unsuccessful (Vo, 1998). This may be a result of the mosaic-like pattern of many

burn wounds, with areas of partial thickness injury within areas of full-thickness injury. It is possible that we failed to sample the actual zones of injury in our model and may have only measured the zones of coagulation and stasis. As a result, the zone of hyperemia in this study may have actually been the zone of stasis. If so, the elevated levels of VEGF in this zone suggest that LED, using the combination therapy of 880nm/730nm/670nm, was effective in stimulating angiogenesis in the zone of stasis. This improvement and verification of the burn wound zones could be more rigorously demonstrated by using laser Doppler scanning methods in addition to histological evaluation (Vo, 1998) to determine actual perfusion of the burn wound.

This study, similar to others, demonstrates the importance of NO on wound healing, particularly in its interactions with other cytokines, growth factors, and inflammatory mediators (Papapetropoulos 1997, Frank 1999, Bussolati 2001, Salvemini 1996, Salvemini 1995).

However, NO's role in angiogenesis and wound healing is not clear-cut; it can accelerate or impair wound healing. Others have documented a duality of NO on VEGF, thereby contributing to the rather controversial role of NO in angiogenesis. NO has been shown to have both inhibitory and stimulatory effects on VEGF gene transcription and angiogenesis, depending on the redox state of the cell and the type of cell (Semenza 1992).

While a relationship between VEGF and NO likely exists in wound healing, only recently, has a positive interrelationship between COX-2 and iNOS been suggested. Nitric oxide donors enhance COX-2 expression and PGI<sub>2</sub> production (Salvemini 1996), but NOS inhibitors block LPS stimulated PGE<sub>2</sub> production (Salvemini 1995). In this study, the COX-2 elevation coincides with that of iNOS; COX-2 levels were elevated at postburn day 7 in the control (no LED treatment) group. Treatment, however, with either 880 nm and combination therapy did not result in appreciable changes in COX-2 levels when compared to no treatment (control) at

postburn day 7 as would be expected if a direct relationship between NO and COX-2 existed. Instead, COX-2 levels were highest in the 670 nm treated animals at postburn day 14. Inhibition of iNOS with the selective iNOS inhibitor L-NIL (L-N6- (1-iminoethyl) lysine) could help clarify if a direct relationship between iNOS and COX-2 exists.

Further findings suggest that there are differential effects of wavelengths on wound healing. Treatment with the 730 nm wavelength LED resulted in improved reepithelialization, yet there were decreased numbers of macrophages. Macrophages orchestrate the release of cytokines and stimulate many of the subsequent processes of wound healing. Bacterial debris, such as lipopolysaccharide, activates macrophages to release free radicals and cytokines, such as nitric oxide, cyclooxygenase, and VEGF that mediate angiogenesis and fibroplasia (Witte 1997). Their decreased numbers suggest that while this wavelength may improve reepithelialization, angiogenesis may be adversely affected. Furthermore, the 730 nm LED treatment group had unexpected increases in hair follicle number, confirming hair follicles as sources of stem cells for regenerating epithelium (Jahoda 2001) and potentially the mechanism behind the increased reepithelialization seen in this treatment group.

#### **EFFECT OF WAVELENGTH ON MACROPHAGE PRODUCTION OF VEGF AND NO IN VITRO**

In order to further delineate the role of macrophages in angiogenesis, the in vitro work examined the effect of LED treatment on macrophage production of VEGF and NO. In accordance with other studies, these results support that nitrite levels (an indirect measure of NO production) are positively correlated with VEGF levels (Xiong, 1998, Ramanathan, 2003). In this study, stimulation of macrophages by the combination of the inflammatory mediators, lipopolysaccharide (LPS) and interferon- $\gamma$  (IFN) also resulted in substantially elevated levels of both nitrites and VEGF (Xiong, 1998, Ramanathan, 2003).

This study demonstrates that unstimulated RAW 264.7 cells respond to two LED treatments (880 nm and combined wavelengths) by increasing cellular VEGF and NO production. Substantially increased growth factor production was noted with both the isolated 880 nm wavelength at  $4\text{J}/\text{cm}^2$ , and the combination treatment (880 nm/730 nm/670 nm) at  $12\text{J}/\text{cm}^2$ . As with our *in vivo* findings, it is not completely clear whether the increased production of pro-angiogenic growth factors that occurred with the combination therapy was due to the sequence of the individual wavelengths or the contribution of increased energy fluence. The 880 nm wavelength appears to be the most promising single wavelength even at the lower energy fluence of  $4\text{J}/\text{cm}^2$ . These findings suggest that using the single 880 nm wavelength at greater energy fluence, such as  $8\text{-}12\text{J}/\text{cm}^2$ , may result in increased production of VEGF and NO and would be beneficial. Whelan et al. (Whelan, 2000) corroborate this dose-dependent effect of energy fluence on cell proliferation, by demonstrating increased cell proliferation as a result of single wavelength (670 nm) therapy at  $8\text{J}/\text{cm}^2$  when compared to  $4\text{J}/\text{cm}^2$ , with a plateau effect at higher energy fluences ( $12\text{J}/\text{cm}^2$ ).

In this study, the ratio of VEGF to NO was substantially less in LPS/IFN-stimulated RAW 264.7 macrophages than in their nonstimulated counterparts. In non-LPS/IFN-stimulated cells, greater changes in VEGF were seen with smaller changes in NO (nitrites). The role of nitric oxide in the inflammatory response and its deleterious effects on all cells including those necessary for normal wound healing progression are well-known (Moncada 1999). In fact, acute injury, such as a large burn, results in activation of macrophages and release of large amounts of nitric oxide, which has been associated with local and systemic inflammatory responses, even on non-injured tissue (Oliveira, 2004). Oliveira et al. found that burn and inhalation injury resulted in increased levels of NO and its metabolites in non-injured skin

(Oliveira, 2004), confirming the importance of NO in mediating the skin response to a burn.

Therefore, while low levels of NO are required to facilitate VEGF signal transduction, higher concentrations (antimicrobial levels) may adversely affect wound healing by prolonging inflammation. We found that LED photostimulation at 880 nm and combination induced lower levels of nitrites and higher levels of VEGF in cells that were not prestimulated with LPS/IFN. In contrast, cells that were prestimulated with LPS/IFN did not produce increased amounts of NO or VEGF in response to LED. These findings suggest that nitrite and VEGF production in the non-LPS/IFN stimulated cells require alternate pathways to that for the LPS/IFN stimulated cells. Xiong, and Ramanathan also found that the pathways involved in the regulation of VEGF production in nonactivated and activated RAW cells were different (Xiong 1996, Ramanathan 2003).

The decreased proliferation of macrophages treated with both LPS/IFN stimulation and LED treatment also suggest that in these groups there is stimulation of inflammatory factors, possibly even an overproduction of reactive oxygen species in addition to NO, leading to cytotoxicity of the macrophages themselves.

While we did not identify this reactive oxygen species, peroxynitrite ( $\text{ONOO}^-$ ) is a likely candidate. Peroxynitrite is a highly oxidant species that is extremely cytotoxic and is formed by NO's interaction with superoxide (SOD) (Moncada 1999). Its presence in burn wounds has most recently been documented by Oliveira et al. who found increased peroxynitrite levels in unburned sheep skin after burn and inhalation injuries (Oliveira, 2004). Their findings confirmed that the effects of an acute burn injury are not just local to the area of the burn itself but also on skin distant from the burn, which can result in progression of the burn.

The effect of peroxynitrite and NO can be severe. Studies in endotoxemic rats (King 1999) and cytokine-stimulated cells via NO and peroxynitrite-dependent mechanisms (Khan 2002) suggest that NO or peroxynitrite may be responsible for derangements in cellular respiration. The mechanism of nitric oxide inhibition of cellular respiration is believed to be at the level of the mitochondria, by affecting cytochrome c oxidase, the last enzyme in the respiratory cycle. Work by Clementi et al. (Clementi 1998) demonstrated that NO at physiological concentrations selectively and reversibly inhibits cytochrome c oxidase (complex IV). However, if NO is produced either in large quantities or for a prolonged period, it will inhibit cytochrome c oxidase irreversibly, preventing oxygen displacement of NO from the enzyme. This results in mitochondrial superoxide production and subsequent peroxynitrite production, leading to irreversible blocking of complex I and III of the electron transport chain (Clementi 1998). In this study, LED-induced NO production in nonLPS/IFN-stimulated cells was much less than that of cells prestimulated with LPS/IFN. It is likely that cells receiving LPS/IFN stimulation responded by producing such large levels of NO that cytochrome c was irreversibly blocked, preventing stimulation by LED.

Treatment with the 730nm LED resulted in decreased VEGF and nitrite levels in both LPS/IFN stimulated and nonstimulated cells suggesting that this wavelength adversely affects macrophage production of VEGF. This finding is in accordance with our in vivo findings with decreased macrophage numbers in burn wounds treated with the 730nm LED. These findings also indicate that there may be a minimal threshold level of NO required for VEGF production.

These in vitro findings corroborate our in vivo findings that light-emitting diode therapy may have vulnerary effects on angiogenesis, specifically by affecting macrophage production of VEGF and NO. These effects appear to be wavelength dependent and appear to be greater as

the wavelength increases, with the 880 nm group having a greater effect than either 730 nm or 670 nm. Our results in the non-LPS/IFN-stimulated and stimulated macrophages also suggest that LED at specific wavelengths can stimulate macrophage production of proliferative factors without stimulating inflammatory factors.

## **CHAPTER 8: CONCLUSIONS**

Our data suggest that LED therapy is beneficial for burn wound healing and warrants additional investigation. LED at 880 nm and the combination of 670,730 and 880 nm may stimulate angiogenesis by increasing the production of VEGF and nitrites. The in vitro findings were confirmed with the in vivo work. Although LED at 880 nm and combination of 670, 730, and 880 nm increase production of VEGF and iNOS, LED at 730 nm increases epithelialization. Thus, differential effects on wound healing may be achieved by varying the wavelengths and fluence of LED photostimulation. Additional investigations will need to be conducted to determine optimal intensities and to standardize treatment parameters.

## CHAPTER 9: BIBLIOGRAPHY

- Akcaay MN, Ozcan O, Gundogdu C, et al. Effect of nitric oxide synthase inhibitor on experimentally induced burn wounds. *J Trauma* 2000; 49: 327-330.
- Al-Watban FAH, Delgado GD. Burn healing with a diode laser: 670 nm at different doses as compared to a placebo group, *Photomedicine Laser Surg* 23(3): 245-250, 2005.
- Andrzejewska E, Niewiadomska H. Evaluation of selected parameters of the cytokine system in burn wounds in children. *Pediatr Surg Int* 2000; 16: 80-84.
- Barbul A. Cytokines. In: Cohen IK, Diegelmann RF, Lindblad WJ, eds. *Wound Healing: Biochemical & Clinical Aspects*. Philadelphia: W.B. Saunders. 1992; 282-291.
- Battal MN, Hata Y, Matsuka K, et al. Reduction of progressive burn injury by a stable prostaglandin I<sub>2</sub> analogue, beraprost sodium (Procylin): an experimental study in rats. *Burns* 1996; 22:531-538.
- Bayat M, Vasheghani MM, Razavi N, et al. Effect of low-level laser therapy on the healing of second-degree burns in rats: a histological and microbiological study, *J Photochem Photobiol B: Biol* 78: 171-177, 2005.
- Blomme EAG, Chinn KS, Hardy MM, et al. Selective cyclooxygenase-2 inhibition does not affect the healing of cutaneous full-thickness incisional wounds in SKH-1 mice. *Br J Dermatol*. 2003; 148(2): 211-23.
- Boykin JV, Eriksson E, Pittman RN. In vivo microcirculation of a scald burn and the progression of postburn dermal ischemia. *Plast Reconstr Surg* 1980; 66:191-198.
- Boykin JV, Molnar JA. Burn scar and skin equivalents. In: Cohen IK, Diegelmann RF, Lindblad WJ, eds. *Wound Healing: Biochemical & Clinical Aspects*. Philadelphia: W.B. Saunders. 1992:523-540.
- Brigham PA, McLoughlin E. Burn incidence and medical care use in the United States: estimates, trends, and data sources. *J Burn Care Rehabil* 1996; 17:95-107.
- Bussolati B, Dunk C, Grohman M, et al. Vascular endothelial growth factor receptor-1 modulates vascular endothelial growth factor mediated angiogenesis via nitric oxide. *Am J Pathol* 2001; 159:993-1008.
- Chai J, Sheng Z, Yang H, et al. Successful treatment of invasive burn wound infection with sepsis in patients with major burns. *Chinese Med J* 2000; 113(12): 1142-1146.

Clementi E, Brown GC, Feelisch M, et al. Persistent inhibition of cell respiration by nitric oxide: crucial role of S-nitrosylation of mitochondrial complex I and protective action of glutathione. *Proc Natl Acad Sci U S A* 1998; 95:7631-6.

Conlan MJ, Rapley JW, Cobb CM. Biostimulation of wound healing by low-energy laser irradiation. A review. *J Clin Periodontol* 1996; 23:492-496.

Crowther M, Brown NJ, Bishop ET, et al. Microenvironmental influence on macrophage regulation of angiogenesis in wounds and malignant tumors. *J Leukoc Biol* 2001; 70: 478-490.

deCamara DL, Raine TJ, London MD, et al. Progression of thermal injury: a morphologic study. *Plast Recon Surg* 69(3): 491-499, 1982.

Del Beccaro EJ, Robson MC, Hegggers JP, et al. The use of specific thromboxane inhibitors to preserve dermal microcirculation after burning. *Surgery* 87(2): 137-141, 1980.

Detmar M, Brown LF, Berse B, et al. Hypoxia regulates the expression of vascular permeability factor/vascular endothelial growth factor (VPF/VEGF) and its receptors in human skin. *J Invest Dermatol* 1997; 108:263-8.

Dulak J, Jozkowicz A, Dembinska-Kiec A, et al. Nitric oxide induces the synthesis of vascular endothelial growth factor by rat vascular smooth muscle cells. *Arterioscler Thromb Vasc Biol* 2000; 20:659-66.

Eells JT, Wong-Riley MT, VerHoeve J, et al. Mitochondrial signal transduction in accelerated wound and retinal healing by near-infrared light therapy. *Mitochondrion* 2004; 4(5-6): 559-67.

Fife RS, Stott B, Carr RE. Effects of a selective cyclooxygenase-2 inhibitor on cancer cells in vitro. *Cancer Biol Ther* 2004; 3:228-232.

Fosslien E. Molecular pathology of cyclooxygenase-2 in neoplasia. *Ann Clin Lab Sci.* 2000; 30(1): 3-21.

Frank S, Stallmeyer B, Kampfer H, et al. Nitric oxide triggers enhanced induction of vascular endothelial growth factor expression in cultured keratinocytes (HaCaT) and during cutaneous wound repair. *Faseb J* 1999; 13:2002-2014.

Futagami A, Ishizaki M, Fukuda Y, et al. Wound healing involves induction of cyclooxygenase-2 expression in rat skin. *Lab Invest.* 2002; 82(11): 1503-13.

Herndon DN, Spies M. Modern burn care. *Semin Pediatr Surg* 2001; 10:28-31.

Isik S, Sahin U, Ilgan S, et al. Saving the zone of stasis in burns with recombinant tissue-type plasminogen activator (r-tPA): an experimental study in rats. *Burns* 1998; 24:217-223.

Jahoda CA, Reynolds AJ. Hair follicle dermal sheath cells: unsung participants in wound healing. *Lancet* 2001; 358:1445-1448.

Jones M, Wang H, Peskar B, et al. Inhibition of angiogenesis by nonsteroidal anti-inflammatory drugs: Insight into mechanisms and implications for cancer growth and ulcer healing. *Nature Medicine* 1999; 5(12): 1418-1423.

Kampfer H, Brautigam L, Geisslinger G, et al. Cyclooxygenase-1-coupled prostaglandin biosynthesis constitutes an essential prerequisite for skin repair. *J Invest Dermatol* 2003; 120(5): 880-890.

Karu T. Photobiology of low-power laser effects. *Health Phys* 1989; 56:691-704.

King CJ, Tytgat S, Delude RL, et al. Ileal mucosal oxygen consumption is decreased in endotoxemic rats but is restored toward normal by treatment with aminoguanidine. *Crit Care Med* 1999; 27:2518-24.

Khan AU, Delude RL, Han YY, et al. Liposomal NAD(+) prevents diminished O<sub>2</sub> consumption by immunostimulated Caco-2 cells. *Am J Physiol Lung Cell Mol Physiol* 2002; 282:L1082-91.

Klein RD, Su GL, Aminlari A, et al. Skin lipopolysaccharide-binding protein and IL-1beta production after thermal injury. *J Burn Care Rehabil* 2000; 21(4): 345-352.

Leong M, Phillips LG. Wound Healing. In: Townsend, Beauchamp, Evers, & Mattox eds: *Sabiston Textbook of Surgery: The Biological Basis of Modern Surgical Practice*. 17<sup>th</sup> edition, Philadelphia, Saunders (Elsevier Science), 2004: 183-207.

Levy RM, Prince JM, Billiar TR. Nitric oxide: a clinical primer, *Crit Care Med* 33(12-Suppl): S492-S495, 2005.

Lorsbach RB, Murphy WJ, Lowenstein CJ, et al. Expression of nitric oxide synthase gene in mouse macrophages activated for tumor cell killing. Molecular basis for the synergy between interferon-gamma and lipopolysaccharide. *J Biol Chem* 1993; 268 (3): 1908-1913.

Mauel J, Ransijn A, Corradin SB, et al. Effect of PGE<sub>2</sub> and of agents that raise cAMP levels on macrophage activation induced by IFN-gamma and TNF-alpha. *J Leukoc Biol* 1995; 58: 217-24.

Mester E, Spiry T, Szende B, et al. Effect of laser rays on wound healing, *Am J Surg*. 122: 532-535, 1971.

Miura S, Tatsuguchi A, Wada K, et al. Cyclooxygenase-2-regulated vascular endothelial growth factor release in gastric fibroblasts. *Am J Physiol Gastrointest Liver Physiol* 2004; 287:G444-451.

Moncada S. Nitric oxide: discovery and impact on clinical medicine. *J R Soc Med* 1999; 92:164-9.

- Morris RJ, Liu Y, Marles L, et al. Capturing and profiling adult hair follicle stem cells. *Nat Biotechnol* 2004; 22:411-417.
- Most D, Efron DT, Shi HP, et al. Differential cytokine expression in skin graft healing in inducible nitric oxide synthase knockout mice. *Plast Reconstr Surg* 2001; 108: 1251-1259.
- Nwomeh BC, Liang H, Cohen IK, et al. MMP-8 is the predominant collagenase in healing wounds and nonhealing ulcers. *J Surg Res* 1999; 81: 189-195.
- Oliveira GV, Shimoda K, Enkhbaatar P, et al. Skin nitric oxide and its metabolites are increased in nonburned skin after thermal injuries. *Shock* 22(3): 278-282, 2004.
- Papapetropoulos A, Garcia-Cardena G, Madri JA, et al. Nitric oxide production contributes to the angiogenic properties of vascular endothelial growth factor in human endothelial cells. *J Clin Invest* 1997; 100:3131-9.
- Papillion P, Valiulis J, Cunningham M, et al. The effect of 810 nanometer diode laser irradiation on healing of full thickness skin wounds in rats. *Wounds* 2004; 16:355-358.
- Ramanathan M, Giladi A, Leibovich SJ. Regulation of vascular endothelial growth factor gene expression in murine macrophages by nitric oxide and hypoxia. *Exp Biol Med* 2003; 228: 697-705.
- Raschke WC, Baird S, Nakoinz PRI. Functional macrophage cell lines transformed by abelson leukemia virus. *Cell* 15(1): 261-267, 1978.
- Raspollini MR, Amunni G, Villanucci A, et al. COX-2 status in relation to tumor microvessel density and VEGF expression: Analysis in ovarian carcinoma patients with low versus high survival rates. *Oncol Rep.* 2004; 11(2): 309-13
- Reddy GK, Stehno-Bittel L, Enwemeka CS. Laser photostimulation accelerates wound healing in diabetic rats. *Wound Repair Regen* 2001; 9:248-255.
- Robson MC, Del Beccaro EJ, Heggors JP, et al. Increasing dermal perfusion after burning by decreasing thromboxane production. *J Trauma* 20(9): 722-725, 1980.
- Robson MC, Del Beccaro EJ, Heggors JP. The effect of prostaglandins on the dermal microcirculation after burning, and the inhibition of the effect by specific pharmacological agents. *Plast Reconstr Surg* 1979; 63:781-787.
- Robson MC, Kucan JO, Paik KI, et al. Prevention of dermal ischemia after thermal injury. *Arch Surg* 113(5): 621-625, 1978.

Rochkind S, Rousso M, Nissan M, et al. Systemic effect of low power laser irradiation on peripheral and central nervous system, cutaneous wounds, and burns, *Lasers Surg Med*: 174-182, 1989.

Salvemini D, Currie MG, Mollace V. Nitric oxide-mediated cyclooxygenase activation. A key event in the antiplatelet effects of nitrovasodilators. *J Clin Invest* 1996; 97:2562-2568.

Salvemini D, Settle SL, Masferrer JL, et al. Regulation of prostaglandin production by nitric oxide; an in vivo analysis. *Br J Pharmacol* 1995; 114:1171-1178.

Sautebin L, Ialenti A, Lanaro A, et al. Modulation of Nitric Oxide of Prostaglandin Biosynthesis in the Rat. *Br J Pharmacol* 1995; 114:323-8.

Schaffer MR, Tantry U, Barbul A. Wound fluid inhibits wound fibroblast nitric oxide synthesis. *J Surg Res* 2004; 122:43-48.

Schlager A, Kronberger P, Petschke F, et al. Low-Power Laser Light in the healing of burns: a comparison between two different wavelengths (635 nm and 690 nm) and a placebo group. *Lasers Surg Med* 2000, 27; 39-42.

Semenza GL, Wang GL. A nuclear factor induced by hypoxia via de novo protein synthesis binds to the human erythropoietin gene enhancer at a site required for transcriptional activation. *Mol Cell Biol* 1992; 12:5447-5454.

Shakespeare P. Burn wound healing and skin substitutes. *Burns* 2001; 27:517-522.

Sliney D, Wolbarsht M. Optical radiation hazards to the skin, in safety with lasers and other optical sources. New York: Plenum Press. 1980. 161-185

Stadler I, Lanzafame RJ, Oskoui P, et al. Alteration of skin temperature during low-level laser irradiation at 830 nm in a mouse model, *Photomedicine Laser Surg* 22(3): 227-231, 2004.

Tarpey MM, Fridovich I. Methods of detection of vascular reactive species: nitric oxide, superoxide, hydrogen peroxide, and peroxynitrite. *Circ Res* 2001; 89:224-236.

Tetsuka T, Daphna-Iken D, Miller B, et al. Nitric Oxide Amplifies Interleukin 1-induced Cyclooxygenase-2 Expression in Rat Mesangial Cells. *J Clin Invest* 1996; 97 (9): 2051-2056

Tripp CS, Blomme EA, Chinn KS, et al. Epidermal COX-2 induction following ultraviolet irradiation: suggested mechanism for the role of COX-2 inhibition in photoprotection. *J Invest Dermatol*. 2003; 121(4): 853-61.

Vindenes HA, Ulvestad E, Bjerknes R. Concentrations of cytokines in plasma of patients with large burns: their relation to time after injury, burn size, inflammatory variables, infection, and outcome. *Eur J Surg* 1998; 164(9): 647-656.

Vo LT, Papworth GD, Delaney PM, et al. A study of vascular response to thermal injury on hairless mice by fibre optic confocal imaging, laser doppler flowmetry and conventional histology. *Burns* 1998; 24:319-324.

Whelan HT, Buchmann EV, Whelan NT. NASA light emitting diode medical applications from deep space to deep sea. *Space Tech Appl* 2001; 552:35-45.

Whelan HT, Houle JM, Whelan NT, et al. The NASA light-emitting diode medical program progress in space flight and terrestrial applications. *Space Tech Appl* 2000; 504:37-43.

Witte MB, Barbul A. General principles of wound healing. *Surg Clin North Am* 1997; 77:509-528.

Wong-Riley MT, Liang HL, Eells JT, et al. Photobiomodulation directly benefits primary neurons functionally inactivated by toxins: role of cytochrome c oxidase. *J Biol Chem* 2005; 280:4761-4771.

Wong-Riley MTT, Bai X, Buchmann E, et al. Light-emitting diode treatment reverses the effect of TTX on cytochrome c oxidase in neurons, *NeuroReport* 12(14): 3033-3037, 2001.

Xiong M, Elson G, Legarda D, et al. Production of vascular endothelial growth factor by murine macrophages: regulation by hypoxia, lactate, and inducible nitric oxide synthase pathway. *Am J Pathol* 1998; 153: 587-598.

Yamada Y, Endo S, Inada K. Plasma cytokine levels in patients with severe burn injury – with reference to the relationship between infection and prognosis. *Burns* 1996; 22(8): 587-593.

Zawacki BE. Reversal of capillary stasis and prevention of necrosis in burns. *Ann Surg* 1974, 180(1): 98-102.

Zhang B, Huang YH, Chen Y, et al. Plasma tumor necrosis factor-alpha, its soluble receptors and interleukin-1beta levels in critically burned patients. *Burns* 1998; 24: 599-603.

## VITA

Mimi Leong was born on May 25, 1968 to Willie (Aung Win) and Khin Kyi Leong in Rangoon, Burma. At the age of 3, Mimi left Burma with her family and settled in San Francisco, California. She received her Bachelor's of Science in Biochemistry at the University of California, Davis where she was an University of California Regents' Scholar and graduated with honors. Mimi's Doctorate of Medicine was earned at the Medical College of Pennsylvania in Philadelphia, Pennsylvania. Following her medical education, Mimi completed her residencies in General Surgery and Plastic Surgery.

While at graduate school, Mimi received several honors. In 2002, Mimi was awarded the Plastic Surgery Educational Foundation / Fresh Start Surgical Gifts Research Fellowship and the Plastic Surgery Educational Foundation Research Grant. Mimi was also awarded the Young Investigator Award Winner in 2004 by the Wound Healing Society.

Mimi served as a mentor for several medical students and undergraduate students, by participating in the Medical Student Summer Research Program and the Summer Undergraduate Research Program while at the University of Texas Medical Branch. She was also asked to participate in these summer research programs as a judge for the scientific poster sessions.

Mimi is currently an Assistant Professor in the Division of Plastic Surgery at Baylor College of Medicine.

### **Education**

B.S., June 1990, The University of California, Davis, CA

M.D., May 1994, The Medical College of Pennsylvania, Philadelphia, PA

July 1994-June 1996, July 1998-June 1999, General Surgery Residency, MCP-Hahnemann University, Philadelphia, PA

July 1996-June 1998, General Surgery Research Fellowship, MCP-Hahnemann University, Philadelphia, PA

July 1999-June 2001, General Surgery Residency, The University of Texas Health Sciences Center, San Antonio, TX

November 2001-June 2003, Plastic Surgery Research Fellowship, The University of Texas Medical Branch, Galveston, TX

July 2003-June 2005, Plastic Surgery Residency, The University of Texas, Houston, TX

## **Publications**

Gould, LJ, Leong M, Sonstein, J, Wilson S. Optimization and validation of an ischemic wound model. *Wound Repair and Regen* 2005; 13(6): 576-582.

Leong M, Phillips, LG. WOUND HEALING. In: TOWNSEND, Beauchamp, Evers & Mattox: SABISTON TEXTBOOK OF SURGERY: The Biological Basis of Modern Surgical Practice. 17<sup>th</sup> edition, Philadelphia, Saunders (Elsevier Science) 2004: 183-207.

Leong M, Granick MS. Microvascular tissue transfer in a pregnant patient. *Journal of Reconstructive Microsurgery* 1998; 14(6): 411-416.

Leong M, Wargo JA, Blankenhorn EP, Murasko DM, Kahng KU. Increased activity of inducible nitric oxide synthase after bile duct ligation in the rat is independent of cyclooxygenase-2 activity. *Surgical Forum* 1998; 49: 168-171.

Leong M, Liu T, Wargo JA, Murasko DM, Kahng KU. Decreased proliferative response in rat splenocytes after bile duct ligation (BDL) is mediated by increased nitric oxide (NO) production. *Surgical Forum* 1997; 48: 197-199.